The Nelson Mandela AFrican Institution of Science and Technology

NM-AIST Repository **https://dspace.mm-aist.ac.tz**

Materials, Energy, Water and Environmental Sciences Masters Theses and Dissertations

2019-02

Investigation of combination effect of natural dye (crocetin) and synthetic dye (indoline d205) for dye sensitized solar cells application

Msangi, Abdala

NM-AIST

https://doi.org/10.58694/20.500.12479/272

Provided with love from The Nelson Mandela African Institution of Science and Technology

INVESTIGATION OF COMBINATION EFFECT OF NATURAL DYE (CROCETIN) AND SYNTHETIC DYE (INDOLINE D205) FOR DYE SENSITIZED SOLAR CELLS APPLICATION

Abdala Msangi

A Dissertation Submitted in Partial Fulfillment of the Requirements for the Degree of Master's in Materials Science and Engineering of The Nelson Mandela African Institution of Science and Technology

Arusha, Tanzania

February, 2019

ABSTRACT

Dye-sensitized solar cells (DSSCs) are reckoned as emerging next-generation solar cells of a high potency. Co-sensitization of dyes facilitates widening of the light absorption range of a sensitizer and is one of possible options to improve overall DSSC performance. In this work, an effect of combination of the natural crocetin dye and synthetic metal free indoline D205 dye was studied. Molecular design of a complex formed from the individual dyes was attempted. The structures, vibrational and electronic spectra of the species were computed by DFT and TD-DFT B3LYP5 methods with mid-sized basis sets. The UV-vis absorption spectra were measured for individual dyes and their mixtures in chloroform solutions. Electron density distribution of the frontier molecular orbitals and energy levels alignment were used for analysis of the electronic spectra and mechanism of transitions. The results indicated that the designed complex can be considered as a potential candidate for DSSCs application with improved properties compared to the individual dyes.

DECLARATION

I, **Abdala Msangi** do hereby declare to the Senate of The Nelson Mandela African Institution of Science and Technology that this dissertation is my own original work and that it has neither been submitted nor being concurrently submitted for degree award in any other institution.

Msangi ..... 07/03/2019 .....

Abdala Msangi

Name and signature of candidate **Date**

The above declaration is confirmed by

Pogrebnoi ..... 07/03/2019 .....

Prof. Alexander M. Pogrebnoi

Name and signature of supervisor **Date**

COPYRIGHT

This dissertation is copyright material protected under the Berne Convention, the Copyright Act of 1999 and other international and national enactments, in that behalf, on intellectual property. It must not be reproduced by any means, in full or in part, except for short extracts in fair dealing; for researcher private study, critical scholarly review or discourse with an acknowledgement, without the written permission of the office of Deputy Vice Chancellor for Academics, Research and Innovations, on behalf of both the author and The Nelson Mandela African Institution of Science and Technology.

CERTIFICATION

The undersigned certify that they have read and hereby recommend for examination by The Nelson Mandela African Institution of Science and Technology a dissertation/thesis entitled: *Investigation of Combination Effect of Natural Dye (Crocetin) and Synthetic Dye (Indoline D205) for Dye Sensitized Solar Cells Application,* in (partial) fulfillment of the requirements for the degree of Masters in Materials Science and Engineering of The Nelson Mandela African Institution of Science and Technology.

.....

Prof. Alexander M. Pogrebnoi

Supervisor

ACKNOWLEDGEMENT

I wish to express my appreciation to my supervisor Prof. Alexander Pogrebnoi as well as Prof. Tatiana Pogrebnaya and Dr. Yusufu Abeid Chande Jande for their unlimited support. My special thanks be expressed to my dear parents, relatives and others who laid the fundamental of my pedagogy, though it was hard, but they never gave up to take this heavy weighted burden. May Almighty looks at you with eyes of love.

Also, I wish to extend my sincere thanks to my academic staffs in the department of Materials, Energy Science and Engineering, my classmates with special thanks to Joyce Elisadiki for their supports and advices which were really encouraging and full of knowledge.

DEDICATION

This work is dedicated to:

To my family especially my lovely wife Chiku Rahim Mdee

To my friends

TABLE OF CONTENTS

LIST OF TABLES

LIST OF FIGURES

LIST OF ABBREVIATIONS AND SYMBOLS

vis

Ult

rav

iole

t-

visi

ble

CHAPTER ONE

INTRODUCTION

1.1 Background information

Dye-sensitized solar cells (DSSCs) are devices for conversion of solar energy into electricity based on sensitization of wide band gap semiconductors (O'Regan and Grätzel, 1991; 2003). They are also called Grätzel cells named after their publication in 1991 (Hagfeldt *et al.*, 2010). DSSCs have gained increasing attention for many years now as they present many potential advantages such as flexibility, lightweight, low cost and easy processing. The dye is a key component of the device since its role is to harvest efficiently the light and inject the photogenerated electrons into the semiconductor oxide (Zhou *et al.*, 2011). Many dyes, such as ruthenium complexes, zinc porphyrin and metal-free organic dyes have been extensively studied for this application. However the use of a single sensitizer (dye) is restricted due to wavelength range of light absorption which leads to low efficiency.

DSSCs have been extensively investigated as potential candidates for renewable-energy systems because of their fundamental and scientific importance in the area of energy conversion (Higashijima *et al.*, 2011). Availability of materials, simplicity in fabrication and reasonable efficiency has made DSSCs a promising alternative to conventional silicon-based solar cells due to their potential application for photovoltaic devices (Arjunan and Senthil, 2013; Santhanamoorthi *et al.*, 2013). The use of synthetic dyes in DSSCs provide better efficiency and high durability, but they suffer from several limitations such as higher cost, tendency to undergo degradation, and usage of toxic materials (Shalini *et al.*, 2015). In recent years metal complexes and organic dyes have been synthesized and utilized as sensitizers. The highest efficiency of DSSCs fabricated by Ru-containing compounds absorbed on nanocrystalline TiO_2 reached 11–12% (Chiba *et al.*, 2006; Zhou *et al.*, 2011). Regardless of high efficiency reached these DSSCs use noble metals in them which are considered as a resource that is limited in amount. On the other hand organic dyes, which are also known as metal free organic dyes, result in lower efficiency compared to metal complexes sensitizers. For example double rhodanine indoline dye D149 is reported to have power conversion efficiencies of up to 8% in DSSCs based on TiO_2. Also the same dye produced a promising efficiency (6.1%) when used in combination with ZnO (Rudolph *et al.*, 2015). As it is reported one important target for many studies is to increase the

performance of DSSCs as well as avoiding dyes aggregation (Hamilton, 1977). Dyes aggregation may lead to molecules residing in the system that are not functionally attached to the TiO_2 surface and act as filters (Khazraji *et al.*, 1999; Ito *et al.*, 2008). It is reported that some ruthenium complexes have shown the best results using chenodeoxycholic acid (CDCA), which functions as an anti-aggregation reagent to improve the photovoltaic effect (Kay and Graetzel, 1993). On the other side, indoline dyes and coumarin dyes form photoactive aggregates on nanocrystalline-TiO_2 electrodes for DSSCs, known as J-aggregation (Sayama *et al.*, 2002; Horiuchi *et al.*, 2004). In order to control the aggregation between dye molecules, indoline dye, D205 was designed by introducing an n-octyl substitute onto the rhodanine ring of D149 for use in DSSCs. The indoline dye, D205 gave 7.2% conversion efficiency using an ionic-liquid electrolyte (Kuang *et al.*, 2008).

Organic dyes have often presented problems as well, such as complicated synthetic routes and low yields. Nevertheless, the natural dyes found in flowers, leaves, and fruits can be extracted by simple procedures. Due to their cost efficiency, non-toxicity, and complete biodegradation, natural dyes have been a popular subject of research (Kuang *et al.*, 2007). Apart from that, several natural dyes have been utilized as sensitizers in DSSCs such as cyanin, carotene, tannin, and chlorophyll (Gómez-Ortíz *et al.*, 2010). The main problem for natural dye is its low efficiency. For example, chlorophyll from spinach is reported to have efficiency of 0.538% (Syafinar *et al.*, 2015). Optimization of the structure of natural dyes to improve efficiency is a promising process.

For the organic dyes structure to be considered as a synthesizer in DSSCs it must contain anchoring groups like carboxylic and cyanoacrylic acids, pyridine groups, phosphonic acid groups, tetracyanate groups, pyridine-N-oxide groups, sulfonic acid groups, and boronic acid groups, which will attach/chelate on the surface of the titanium dioxide or zinc oxide semiconductors (Zhang and Cole, 2015).

1.2 Working principle of DSSCs

In the first stage, the absorption of the sunlight photons *hv* starts at the dye (D) molecules and electrons (e^-) in the dye get excited from the highest occupied molecular orbital (HOMO) to lowest unoccupied molecular orbital (LUMO) state (Akila *et al.*, 2016). The description is shown in Fig. 1 and by Eqs.(1-5).

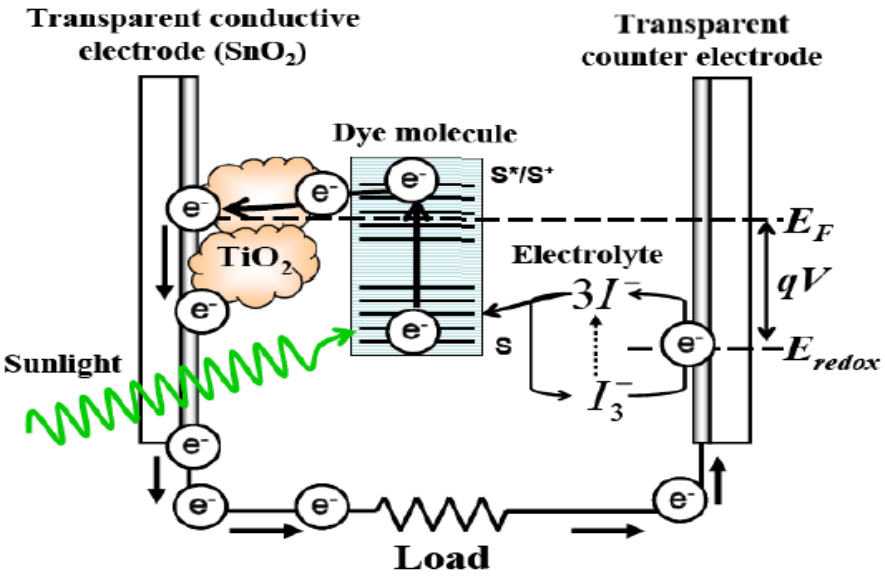

Figure 1: Schematic on how sunlight is converted to electricity in DSSCs (Jasim *et al.*, 2011).

$$D + h\nu \rightarrow D^* \quad (1)$$

After an electron injected from LUMO enters the conduction band of the nanostructure TiO_2 film (the working electrode). This makes the dye molecules become oxidized (Akila *et al.*, 2016)

$$D^* + TiO_2 \rightarrow D^+ + e^-(TiO_2) \quad (2)$$

The electron transported between the TiO_2 nanoparticles will be extracted to a load where the work done is delivered as electrical energy.

$$e^-(TiO_2) + \text{Electrode} \rightarrow TiO_2 + e^-(\text{Electrode}) + \text{Energy} \quad (3)$$

As there is a movement of electrons between the TiO_2 (the working electrode) and the carbon coated counter electrode, electrolyte containing iodide ions I/I_3^- is used to regenerate electrons; it fills the cell

$$D^+ + 2e^- \rightarrow D + I_3^- \quad (4)$$

The I_3^- ions substitutes the donated electron internally with that from the external load and gets reduced back to I^- ion

$$2e^-(\text{Electrode}) + I_3^- \rightarrow 3I^- + \text{Electrode} \quad (5)$$

1.3 Research problem

It is reported that different types of natural dyes show different solar energy conversion efficiencies depending on the source, chemical structure of dye, and interaction between dye molecules and photo-electrode (Hao *et al.*, 2006). Due to the fact that single dye especially natural dyes absorb very small portion of the visible spectrum (Karki *et al.*, 2013) its efficiency is low. For the natural dye to be used in solar cell its efficiency should be enhanced by increasing its absorption range. In order to increase the efficiency of natural dyes the combination of two or more dyes, which have complementary absorption properties in the visible region, may be used for broad responses to the solar spectrum (Kimura *et al.*, 2012). This study is intended for the combination between natural (crocetin) and synthetic (indoline, D205) dyes so as to enhance the performance of the DSSCs.

1.4 Problem justification

Due to the fact that power consumption in the world is constantly increasing, there is a need for a searching for alternative to fossil fuels. These alternative ways should be environment friendly and cost effective (Mphande and Pogrebnoi, 2014). Natural dyes have become a viable alternative to expensive and rare organic sensitizers because of its low cost, easy attainability, abundance in supply of raw materials and no environment threat. Hence there is a high need of utilizing the natural dyes so as to minimize the great use of fossil fuels (Narayan, 2012).

1.5 Significance of the research

Due to depletion of fossil fuels, environment impacts together with high cost of the conventional solar cells, nowadays the potential of DSSCs is increasing. The increase of efficiency of the natural dyes in DSSCs applications due to combination/co-sensitization is a promising result for the future use of these dyes as alternative energy sources. This study gives foundation for the designing of a new sensitizer through a combination of natural and synthetic dyes since that, the new complex may have a high performance compared to the individual dyes. Also this study lays a basis for future studies.

1.6 Objectives

1.6.1 General objective

The general objective of this study is to investigate the effect of combination between natural dye (crocetin) and synthetic dye (indoline, D205) for DSSCs applications.

1.6.2 Specific objectives

(i) Molecular design of complex molecule through combination of the crocetin and indoline D205 dyes;

(ii) To determine the geometrical parameters and vibrational spectra of the dyes (crocetin, tocopherol, retinol and indoline D205) by using quantum chemical methods;

(iii) To compute the electronic spectra of crocetin, tocopherol, retinol and indoline D205 dyes and the complex molecule;

(iv) To measure experimentally UV-vis spectra of solutions of crocetin, tocopherol, retinol and indoline D205 dyes and mixture of crocetin and indoline D205 dyes.

1.7 Research questions

(i) What is the equilibrium geometrical structure of the individual dyes molecules and the complex?

(ii) What are the theoretical vibrational and electronic spectra of crocetin, indoline D205, tocopherol, retinol and the combination of the selected dyes?

(iii) What are the main absorbance bands in UV-vis experimental spectra of the natural, synthetic dye and mixture of selected dyes?

(iv) Is there an agreement between the theoretical and experimental spectra?

(v) What is the energy level alignment of the species considered and semiconductors?

CHAPTER TWO

LITERATURE REVIEW

2.1 Basic requirements to a dye for DSSCs

For a dye to be more efficient in DSSCs applications the following features are very important; the dye must have anchoring group/groups to attach to the semiconductor surface, appropriate alignment of HOMO and LUMO levels which will facilitate charge injection into the semiconductor, dye regeneration from electrolyte, it should absorb light in a broader region of visible and NIR and lastly its photo stability and solubility (Giribabu *et al.*, 2012; Ladomenou *et al.*, 2014). In order to improve the efficiency of dye-sensitized solar cells the above list of requirements has to be fulfilled. Simply by changing the additive (Nazeeruddin *et al.*, 1993; Boschloo *et al.*, 2006) or the redox couple (Yella *et al.*, 2011) in the cell, the energetic of the interface and therefore the electron transfer kinetics is completely changed, and the best dye in some experiment is not necessarily the best in some other. Currently research efforts include so many different directions (synthesis of new dyes, exploration of new electrolytes, hole conducting materials, and additives) that, clearly, there are no established "optimal" components of the DSSCs yet (Ambrosio *et al.*, 2012). Anchoring to TiO_2 or ZnO has been achieved through a number of functional groups, such as salicylate, carboxylic acid, sulphonic acid, phosphonic acid and acetylacetonate derivatives. The most widely used and successful to date being the carboxylic acid and phosphonic acid functionalities (Campbell *et al.*, 2004).

The anchoring group facilitates the attachment of the dye to the semiconductor surface and this determines the binding energy of the dye on TiO_2 or ZnO as well as modulating the injection energy by changing the energy of the dye's excited state. It is reported in the literature (Ambrosio *et al.*, 2012) that the anchoring group of the dye can affect the injection rate into two ways, namely through the electronic coupling between the dye and the semiconductor, mediated by the anchor group, and through the position of the dye's virtual orbital and its energy alignment with the TiO_2 conduction band.

2.2 Types of dyes used in DSSCs

Dye sensitizers serve as solar energy absorbers in DSSCs, which control the light harvesting efficiency and the overall photoelectric conversion efficiency. The sensitizers used in DSSCs are divided into two types: organic dyes and inorganic dyes according to the structure

(Yamazaki *et al.*, 2007). Inorganic dyes include metal complexes, such as polypyridyl complexes of ruthenium and osmium, metal porphyrin, phthalocyanine and inorganic quantum dots, while organic dyes include natural and synthetic organic dyes (Sekar and Gehlot, 2010).

Synthetic organic dyes include metal free dyes such as indoline dyes. Indoline dyes as photosensitizers for DSSCs has been used since 2003, these metal-free organic dyes have increasingly attracted interest due to its promising efficiency, low-cost alternative to Ru(II)-based photosensitizers (Matsui *et al.*, 2016). Especially when adsorbed together with a co-adsorbate like cholic acid (CA) in order to prevent aggregation on the surface of the semiconductor, indoline dyes yield competitive results. One of the most well-known sensitizers of this group, the double rhodanine indoline dye (D149), has produced power conversion efficiencies (η) of up to 8% in DSSCs based on TiO_2. Also the same dye yielded a promising results (η = 6.1%) in combination with ZnO. The main absorption peak of D149 adsorbed to TiO_2 or ZnO is centered around 550 nm and extends no further than to wavelengths of around 620−650 nm, which means that the dye can cover the red part of the solar spectrum (Rudolph *et al.*, 2015). Indoline dye D205, in which the ethyl group in the terminal rhodanine ring of D149 is substituted with an octyl group, has been reported to show an improved open circuit photovoltage (Voc) to give higher conversion efficiency than D149 (Matsui *et al.*, 2016).

Natural dyes can be easily extracted from fruits, vegetables and flowers with minimal chemical procedures (Calogero *et al.*, 2010). Natural dyes may be grouped according to their chemical structures as shown in Fig. 2. Only carotenoids will be described in this work as they contain crocetin which was used in combination with synthetic dye. Carotenoids are usually responsible for petal colors in yellow-to-orange (Kishimoto *et al.*, 2005). Among the two types of carotenoids (crocetin and crocin) crocetin exhibits the best photoelectrochemical performance. The photoelectric conversion efficiency of DSSCs sensitized with crocetin (0.56%) is three times or more as high as that of crocin (0.16%). Regarding its structure, carotenoids have been not given much attention as sensitizers for the DSSCs for two reasons. First, most of the carotenoid species do not have effective functional groups to bond with TiO_2. Secondly, strong steric hindrance of long chain alkane of carotenoid species prevents the dye molecules from arraying on TiO_2 film efficiently. Due to the two reasons, carotenoid

species are not nearly adsorbed on TiO_2 film and sensitizing effect on TiO_2 film tends to be low (Yamazaki *et al.*, 2007).

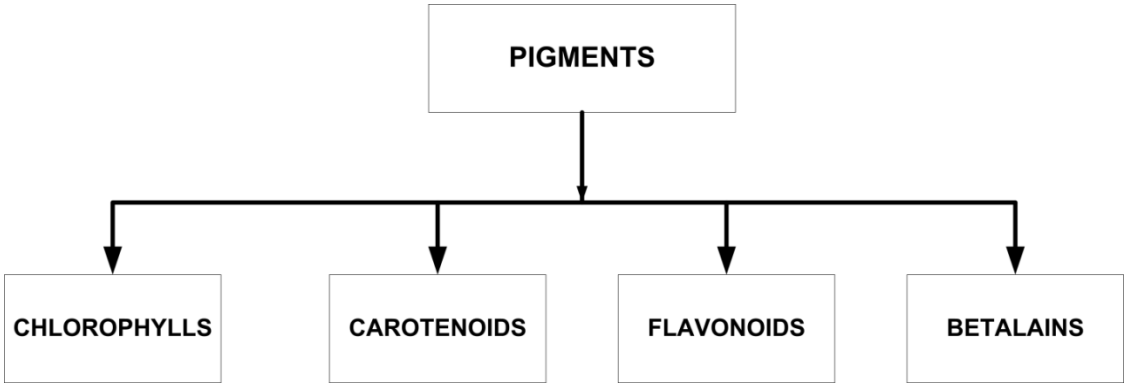

Figure 2: Groups of natural dyes according to their chemical structures.

2.3 Efficiency of DSSCs with natural dyes

Since that time when Grätzel (2003) developed DSSCs, a new type of solar cells have attracted considerable attention due to their advantage of being environmentally friendly and low cost of production. In nature, fruits, flowers and leaves of plants show various colors from red to purple and contain various natural dyes which can be extracted by simple procedures. These dyes can be used as photosensitizers for DSSCs. Many studies have been done on natural dyes as sensitizers of DSSCs (Tennakone *et al.*, 1997) but the efficiency of the natural dye sensitizers was reported to be very low (Dai and Rabani, 2002).

It is reported that a conversion efficiency of 0.66% has been attained using red sicilian orange juice dye as sensitizer (Calogero and Di Marco, 2008). Other researchers utilized rose bengal dye as sensitizer and achieved 2.09% conversion efficiency (Roy *et al.*, 2008). Coumarin derivation dye obtained from structural modification of coumarin as a sensitizer in DSSCs, provided an efficiency of 7.6% (Wang *et al.*, 2005). Thus, optimization of the structure of natural dyes to improve efficiency is promising.

Compared to the well-known silicon devices, DSSCs are belonging to the emerging third-generation photovoltaic concept and use synthetic or natural dyes as light harvesting pigments (Kalyanasundaram, 2010). The currently most efficient Grätzel cells are still much less efficient in comparison to standard silicon-based solar cells. But as a result of the light absorption mechanism of the pigments, DSSCs work even in low-light conditions. Therefore, DSSCs are able to work under cloudy skies and indirect sunlight, whereas inorganic semiconductor-based photovoltaic cells would suffer a cut-off at some lower limit of

illumination. Since the cut-off of DSSCs is so low, they are even proposed for indoor use, collecting energy for small devices from the light inside buildings (Sacco *et al.*, 2013). Eleven natural dyes were extracted from three trees and used as photo sensitizers for DSSCs. These dyes were extracted from the leaves, flowers, barks, and roots of the three trees and TiO_2 was used as a semiconductor. The efficiencies obtained from the DSSCs fabricated using the extracted dyes were as follows; lycium shawii flower (0.10%), olive grain (0.12%), olive leaves (0.17%), lycium shawii leaves (0.32%), zizyphus leaves (0.40%), olive bark (0.06%), lycium shawii bark (0.02%), zizyphus bark (0.07%), olive root (0.08%), lycium shawii root (0.01%) and zizyphus root (0.04%), respectively. DSSCs sensitized with plant leaves showed higher efficiency than those sensitized with other parts of the trees due to the presence of chlorophyll as the absorption spectra showed. The highest conversion efficiency was 0.40% for the DSSC sensitized with zizyphus leaves. DSSCs sensitized with roots and barks exhibited the lowest efficiency (Abdel-Latif *et al.*, 2015).

2.4 Combination of dyes

Many studies have been done in mixing dyes to obtain a wide range of absorption in the visible region. For example (Chang and Lo, 2010) combined anthocyanin and chlorophyll at the ratio of 1:1 to serve as a natural dye mixture from mulberry fruits and pomegranate leaves. The absorption range of chlorophyll dye was in 400–500 nm while the peak for anthocyanin dye was located at 543 nm. The absorption wavelengths of the two dyes are located between 400 and 600 nm. By observing the absorption range of a combination dye, it is found that when two natural dyes are mixed, the absorption range is enhanced, promoting the photoelectric conversion efficiency of a dye-sensitized solar cell. Furthermore it is known that different dyes show different absorption range/wavelength due to different composition (Bisquert and Vikhrenko, 2004; Polo and Iha, 2006). Actually after mixing the two or more dyes, composition might be changed that is why the individual absorption differs from that of the mixture.

By using a combination of natural dyes, efficiency was enhanced up to 0.27% by mixing flame tree flower extract and pawpaw leaf as individually, both flame tree flower extract and pawpaw reached efficiencies of 0.20% (Kimpa *et al.*, 2012). The efficiency of DSSCs with dye extracted from rosella, blue pea flowers and a mixture of these extracts was reported to be 0.37%, 0.05% and 0.15%, respectively. By decreasing the pH value and the extraction

temperature of rosella dye, it was found that the efficiency improved from 0.37% to 0.70% for the DSSC utilizing rosella extract (Wongcharee *et al.*, 2007).

Furthermore the conversion efficiency of the DSSCs prepared by anthocyanin dyes from mulberry extract was 0.548%, while there was a conversion efficiency of 0.722% for chlorophyll and anthocyanin as the dye cocktails (Chang and Lo, 2010).

2.5 Energy level alignment

In order to predict the energy level alignment of dyes calculation of the excited state oxidation potential in relation to the semiconductors conduction band edge is important. Also this calculation is useful for the interpretation of photovoltaic data but represents also a predictive tool for new sensitizers. If the calculated energy difference between the dyes excited state and the semiconductors conduction band edge is too low or negative (*i.e.* the dye excited state lies below the semiconductors conduction band edge) an unfavorable electron injection can be predicted, hence the dye cannot be considered as a sensitizer (De Angelis *et al.*, 2008).

In the TD-DFT study of the electronic properties of dyes the solvent effects should be included on the framework calculations. This is because the effect of solvent in the calculation of the excited states of the dyes is required (Dong *et al.*, 2012) so as to reveal the actual environment of the system, which can give a much better agreement with the experimental values. Many theoretical studies confirm that inclusion of the solvent effects is a crucial factor in describing the absorption spectra of the sensitizers (Guillemoles *et al.*, 2002; Fantacci *et al.*, 2004).

CHAPTER THREE

MATERIALS AND METHODS

3.1 Samples collection

The crocetin and indoline D205 dye samples were purchased in powder form with a stated purity of 97% (HPLC) from MedKoo Biosciences, Inc (USA) and Sigma-Aldrich Chemical Company (USA), respectively; and were used for solution preparation at room temperature.

Tocopherol sample in a liquid form (Tocopherols mixed, FCC, FG) was purchased from Sigma-Aldrich Chemical Company (USA) and had concentration of 0.930 g/mL. Retinol sample in a liquid form was purchased from Shanghai Touch Health Biotechnology Co.,Ltd. All of these samples were used for solutions preparation without further purification.

3.2 Preparation of dye solutions

For crocetin solution preparation, 0.7 mg of the crocetin powder was dissolved in 10 ml (7×10^{-2} g L^{-1}) of chloroform, and then 1 ml of the solution was added to 5 ml of chloroform resulting in 1.4×10^{-2} g L^{-1} concentration. This was used as a sample for crocetin UV-vis spectra measurements. Also for indoline dye D205, 0.5 mg of the sample was dissolved in 50 ml of chloroform resulting in concentration of 10^{-2} g L^{-1}, then 1 ml of this solution was added to 40 ml of chloroform, and the solution of indoline used for UV-vis spectra measurements had the concentration of 2.5×10^{-4} g L^{-1}. For the mixture preparation, 1 ml of indoline dye D205 was added to 1ml of crocetin dye solution and the solvent in all cases was chloroform. This was used as a sample for measurements of UV-vis spectra.

Other natural dyes which were included in our study were retinol and tocopherol. The preparation of these dyes for experimental work was as follows; retinol sample was prepared by mixing 1ml of retinol in 5ml of ethanol. After 30 minutes the sample was taken for UV-vis spectra measurement. After that the sample of tocopherol was prepared by adding 0.5ml of tocopherol in 5ml of ethanol that is 1:1 (v/v) proportions and after 30 minutes the prepared solution were taken into UV-vis spectrophotometer for spectra measurement.

3.3 Geometrical optimization of the species

The density functional theory B3LYP5 with 3-21G basis set was used for the geometrical parameters optimization and computation of vibrational spectra. Geometrical optimization has been done for all species under this study using the stated method while vibrational spectra have been done only for three species, namely crocetin, indoline D205 and the complex. The initial coordinates of the crocetin $C_{20}H_{24}O_4$, indoline D205 $C_{48}H_{47}N_3O_4S_3$, tocopherol ($C_{29}H_{50}O_2$) and retinol ($C_{20}H_{30}O$) molecules were taken from ChemSpider Database (www.chemspider.com). The complex $C_{68}H_{69}N_3O_7S_3$ was designed through combination (etherification reaction) of two molecules, crocetin and indoline D205. For the computation of the complex parameters the same approach, B3LYP5/3-21G, as for the individual dyes was applied. The energy and enthalpy of the complex formation reaction

$$C_{20}H_{24}O_4 + C_{48}H_{47}N_3O_4S_3 = C_{68}H_{69}N_3O_7S_3 + H_2O \quad (1)$$

were computed with different basis sets, from 3-21G to 6-31G(d,p) with geometrical parameters optimized with the 3-21G basis set. The energies of the reaction $\Delta_r E$ were calculated as the difference between the total energies of the product and reactants:

$$\Delta_r E = \Sigma E_{\text{prod}} - \Sigma E_{\text{react}} \quad (2)$$

The enthalpies of the reactions $\Delta_r H°(0)$ were obtained using $\Delta_r E$ and the zero-point vibration energy $\Delta_r \varepsilon$:

$$\Delta_r H°(0) = \Delta_r E + \Delta_r \varepsilon \quad (3)$$

$$\Delta_r \varepsilon = \frac{1}{2} hc(\Sigma \omega_{\text{i prod}} - \Sigma \omega_{\text{i react}}) \quad (4)$$

where h is the Plank's constant, c is the speed of light in the free space, $\Sigma\omega_{i\ \text{prod}}$, and $\Sigma\omega_{i\ \text{react}}$ are the sums of the vibration frequencies of the product and reactants, respectively.

3.4 Electronic spectra of the species

The electronic spectra of the species were calculated at the TD-DFT B3LYP5/6-31G level of theory. The computations were done both for vacuum and solvent (chloroform/ethanol); for solutions the polarized continuum model (PCM) was used. The calculations were performed using the Firefly QC package (Granovsky, 2016), which is partially based on the GAMESS (US) (Schmidt *et al.*, 1993) source code. According to the method implemented the equations have been solved for 6 to 10 excited states. The geometrical structures, vibrational and electronic spectra were visualized and analyzed using the Chemcraft (Zhurko and Zhurko,

2015) and MacMolPlt (Bode and Gordon, 1998) software. In all cases the displayed spectra show the calculated frequencies and absorption wavelengths.

3.5 UV -vis spectra measurement

The UV-vis spectra of the samples prepared have been recorded in the region around 200–800 nm using a single beam 2800 UV-vis spectrophotometer (Hitachi U-2000). The dye samples were diluted for UV-vis measurements. In case of crocetin, indoline D205 and mixure of the two dyes, chloroform was used as a solvent, while for tocopherol and retinol ethanol was used as a solvent. The choice of the solvent to be used for a certain dye was based on the idea of solubility. Measurements of spectra in all cases were taken at the interval of 2nm. All data were processed using excel software.

CHAPTER FOUR

RESULTS AND DISCUSSION

4.1 Molecular structure of individual dyes and complex

Equilibrium geometrical structures of crocetin and indoline molecules are shown in Figs. 3 and 4. In the crocetin, the middle part is composed of four methyl groups, and two carboxylic groups COOH attached at the ends. The molecular structure of the indoline dye D205, comprises diphenylethenyl, bicyclic indoline and two rhodanine groups (Xu *et al.*, 2010). The combination of two dyes through the chemical reaction (1) with elimination of water molecule leads to the formation of the complex; the optimized geometrical structure is shown in Fig. 5. The selected geometrical parameters of the individual dyes are compared with those in the complex molecule in Tables 1 and 2.

In the complex, the joining of the molecules occurs *via* a new chemical bond C19-O3-C23. One can suggest that formation of this bond is accompanied by detachment of the H-atom from H23-O1-C19 fragment of the crocetin (Fig. 3) and hydroxyl O2-H3 from the carboxylic group of the indoline (Fig. 4) to release water molecule. The bond C19-O3-C23 in the complex is specified with parameters *R* (C19-O3) = 1.461 Å, *R* (O3-C23) = 1.385 Å, ∠C19-O3-C23 = 119.2°; which are comparable with those of the ether C-O-C linkage, 1.40 Å and 110°. In the vicinity of the new chemical bond, a slight elongation of the internuclear distances C-O and C=C, by 0.003–0.069 Å, is observed while the bond lengths C=O and C-C are slightly decreased. Generally, from individual dyes to the complex, the difference in the respective parameters is in the range from –0.02 Å to +0.07 Å for bond lengths and ±0.05° for bond angles; bigger change is seen for crocetin moiety. The parameters of the remote parts of the complex remain practically the same as within the individual dyes.

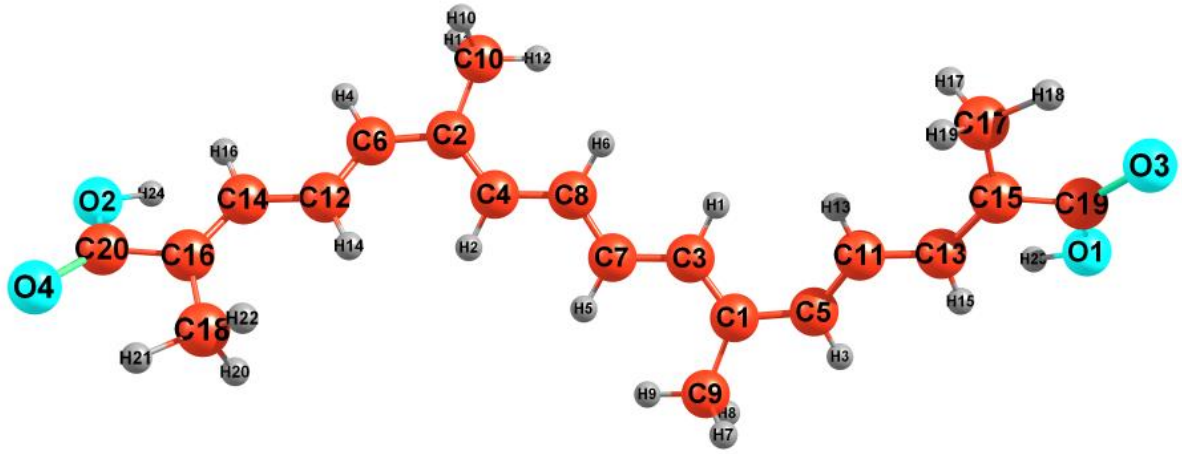

Figure 3: Optimized geometrical structure of the crocetin molecule.

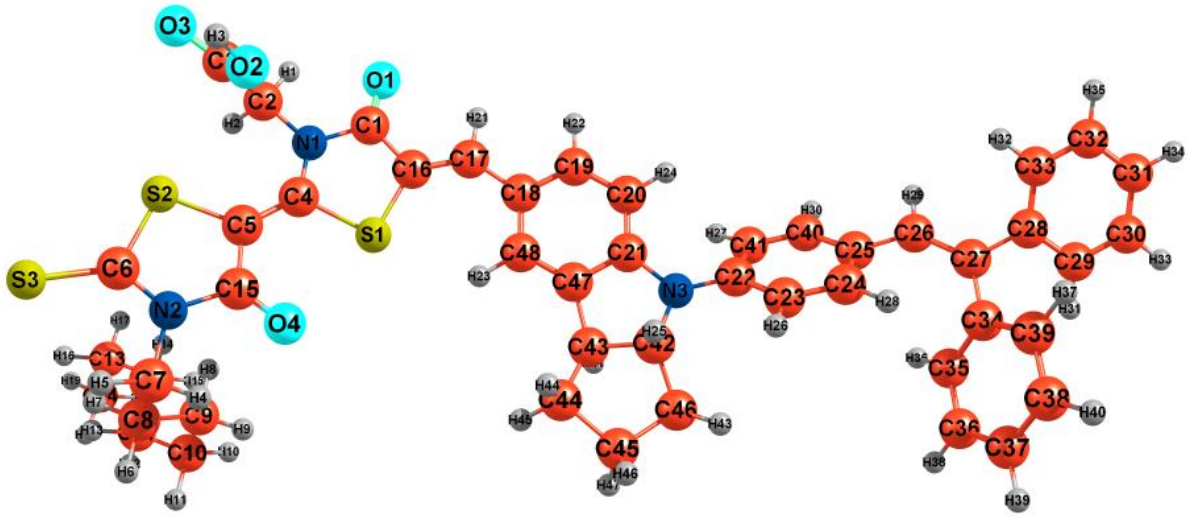

Figure 4: Optimized geometrical structure of the indoline dye D205 molecule.

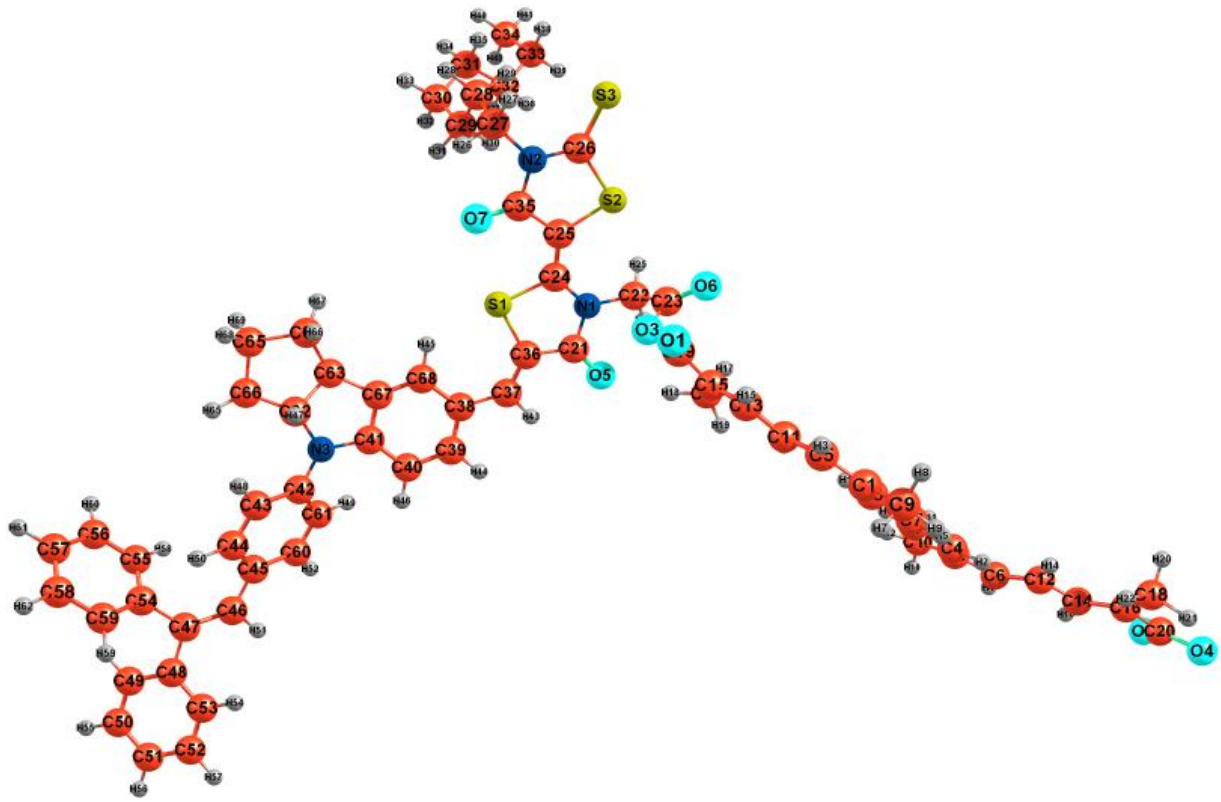

Figure 5: Optimized geometrical structure of the complex molecule.

Table 1: Comparison of selected geometrical parameters in crocetin and complex molecules.

Crocetin		**Complex**		
Bond	Bond lengths, Å	Bond	Bond lengths, Å	Difference
O3=C19	1.226	O1=C19	1.217	–0.009
O1-C19	1.392	O3-C19	1.461	+0.069
		O3-C23	1.385	
C15-C19	1.493	C15-C19	1.470	–0.023
C13=C15	1.356	C13=C15	1.361	+0.005
C11-C13	1.441	C11-C13	1.434	–0.007
C1-C5	1.458	C1-C5	1.455	–0.003
C16-C20	1.493	C16-C20	1.493	0.000
O4=C20	1.226	O4=C20	1.226	0.000
	Bond angles, deg		Bond angles, deg	
O1-C19=O3	119.5	O3-C19=O1	118.8	–0.7
C17-C15-C19	114.5	C17-C15-C19	119.9	+5.4
C13=C15-C19	120.3	C13=C15-C19	114.9	–5.4
C1-C5=C11	127.0	C1-C5=C11	128.3	+1.3
C18-C16-C20	114.5	C18-C16-C20	114.3	–0.2
O2-C20=O4	119.5	O2-C20=O4	119.5	0.0

Table 2: Comparison of selected geometrical parameters in indoline D205 and complex molecules.

Indoline D205		**Complex**		
Bond	Bond lengths, Å	Bond	Bond lengths, Å	Difference
C2-C3	1.523	C22-C23	1.525	+0.002
N1-C2	1.465	N1-C22	1.463	–0.002
C4=C5	1.355	C24 =C25	1.358	+0.003
C1-C16	1.459	C21-C36	1.458	–0.001
C3-O2	1.372	C23-O3	1.385	+0.013
C3=O3	1.222	C23=O6	1.219	–0.003
C1=O1	1.238	C21=O5	1.241	+0.003
C17-C18	1.444	C37-C38	1.444	0.000
C16=C17	1.351	C36=C37	1.352	+0.001
S1-C4	1.848	S1-C24	1.846	–0.002
C19=C20	1.392	C39=C40	1.393	+0.001
C21-N3	1.409	C41-N3	1.407	–0.002
C35=C36	1.398	C55=C56	1.396	–0.002
	Bond angles, deg		Bond angles, deg	
C3-C2-N1	114.4	C23-C22-N1	113.9	–0.5
S2-C6=S3	122.0	S2-C26=S3	121.9	–0.1
C4=C5-S2	127.7	C24=C25-S2	128.1	+0.4
C4-S1-C16	89.7	C24-S1-C36	89.7	0.0
C16=C17-C18	131.5	C36=C37-C38	131.2	–0.3
	Dihedral angles, deg		Dihedral angles, deg	
C15-N2-C6-S3	178.9	C35-N2-C26-S3	179.4	+0.5
S1-C4-C5-S2	178.6	S1-C24-C25-S2	177.2	–1.4

The theoretical study on tocopherol and retinol includes geometry optimization and energy computation using TD-DFT. Experimental study of these two dyes comprises the UV vis spectra measurements where ethanol was used as a solvent. The equilibrium geometrical structures of tocopherol and retinol molecules are shown in Figs. 6 and 7.

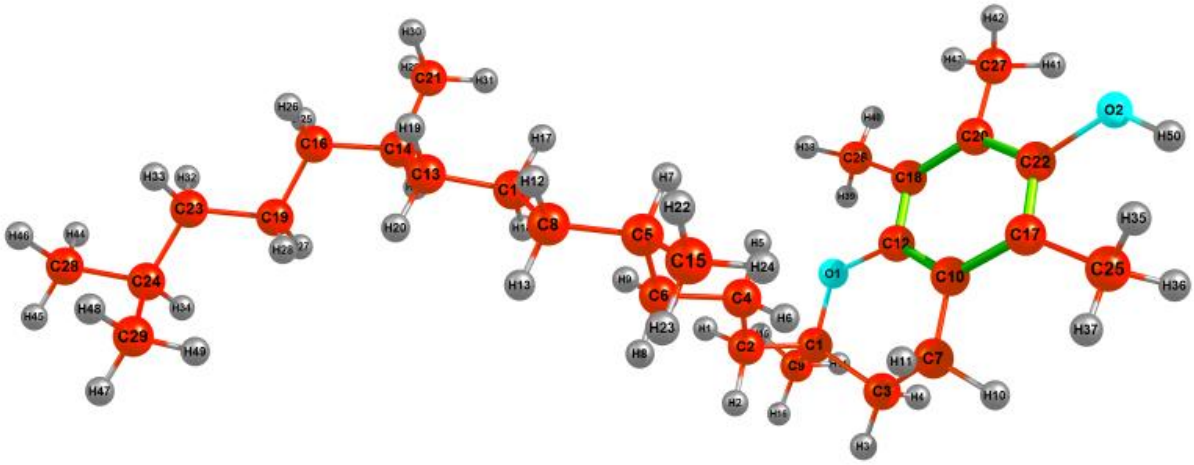

Figure 6: Optimized geometrical structure of the tocopherol molecule.

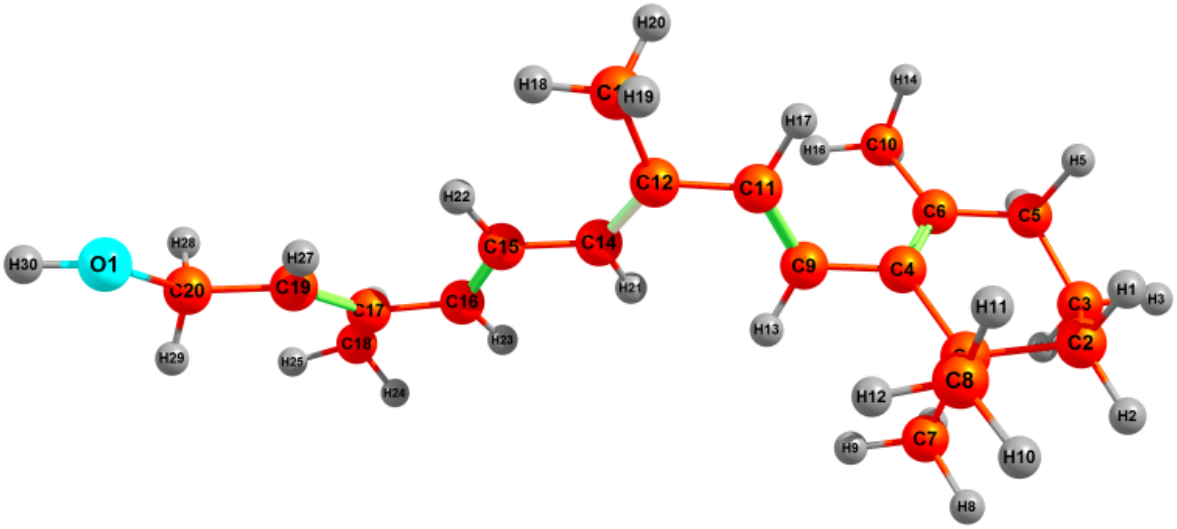

Figure 7: Optimized geometrical structure of the retinol molecule.

4.2 Thermodynamic characteristics of the complex molecule.

The thermodynamic characteristics of the complex formation reaction (1) are given in Table 3. The thermodynamic functions, entropies $S°(T)$ and enthalpy increments $H°(T)–H°(0)$, of the crocetin, indoline, complex and water molecules have been computed with OpenThermo software (Tokarev, 2007-2009); in calculations, the geometrical parameters and vibrational frequencies of the molecules were used as computed with the 3-21G basis set. The Gibbs free energies $\Delta_r G°(T)$ of the reaction were calculated as follows:

$$\Delta_r G°(T) = \Delta_r H°(T) - T\Delta_r S°(T) \qquad (5)$$

where $\Delta_r H°(T)$ and $\Delta_r S°(T)$ are the enthalpy and entropy of the reaction at temperature T; $\Delta_r H°(T) = \Delta_r H°(0) + \Delta_r[H°(T) - H°(0)]$.

Table 3: The thermodynamic characteristics of reaction (1): energy $\Delta_r E$, zero point vibration energy $\Delta_r\varepsilon$, enthalpies $\Delta_r H°(0)$ and $\Delta_r H°(298)$, Gibbs free energy $\Delta_r G°(298)$.

Quantity, kJ mol^{-1}	3-21G	6-31G	6-31G(d,p)
$\Delta_r E$	42.2	41.5	41.9
$\Delta_r\varepsilon$	–8.83	(–8.83)	(–8.83)
$\Delta_r H°(0)$	33.4	32.7	33.1
$\Delta_r H°(298)$	38.1	36.4	36.8
$\Delta_r G°(298)$	48.2	46.5	46.9

The values of $\Delta_r E$ computed with different basis sets do not change noticeably with the basis set extension. Positive values of enthalpies $\Delta_r H°$ show endothermicity of the reaction. The entropy of the reaction is negative, $\Delta_r S°(298) = –33.9$ J mol^{-1} K^{-1}, that points out a rising of the system's order. The Gibbs energy being positive at 298 K shows non-spontaneity of the complex formation through direct combination of the dyes' molecules.

4.3 Vibrational spectra of the crocetin, indoline D205 and complex molecules

Vibrational spectra of the species were calculated by DFT B3LYP5 method with 3-21G basis set. An absence of imaginary frequencies confirmed that the geometrical structures of the species corresponded to minima on the potential energy surfaces. The computed IR spectra are shown in Figs. 8-10. The most intensive modes in the spectra are assigned to the vibrations 1220-1247 cm^{-1} (C-C stretching), 1615-1676 cm^{-1} (C=C stretching), 1115 cm^{-1} (C-O stretching and CH_3 bending), 1764 cm^{-1} (C=O stretching) of the crocetin molecule (Fig. 8), and 1120 cm^{-1} (C-C stretching), 1618-1621 cm^{-1} (C=C stretching), 1156-1188 cm^{-1} (mostly C-N and C-C stretching), 1504 cm^{-1} and 1556 cm^{-1} (H-C-H bending in the six-member ring), 1786 cm^{-1} (C=O stretching) of the indoline molecule (Fig. 9). Comparison of our results to experimental frequencies of crocetin (Schulz and Baranska, 2007), 1536 cm^{-1} (C=C stretching), 1165 cm^{-1} (C-C stretching) and 1020 cm^{-1} (C-C in-plane rocking), shows that our calculated frequencies are overrated by 7-8% which is typical for theoretical results of similar computational level.

Infrared spectrum of the complex (Fig. 10) apparently comprises the intensive modes which correspond to the crocetin moiety (1115 cm^{-1} C-O stretching and CH_3 bending, 1251 cm^{-1} C-C stretching), and indoline moiety (1121 cm^{-1} C-C stretching, 1154 cm^{-1} C-N and C-C

stretching, 1616-1619 cm^{-1} C=C stretching) being shifted slightly from the position in spectra of individual dyes. The frequencies in the range 1760-1790 cm^{-1} relate to stretching vibrations of two C=O groups, one from crocetin and another from indoline part. Also one can see the additional peaks at 960 and 1167 cm^{-1} which are assigned to the C-O stretching motion of atoms in the new bond C19-O3-C23 between the moieties.

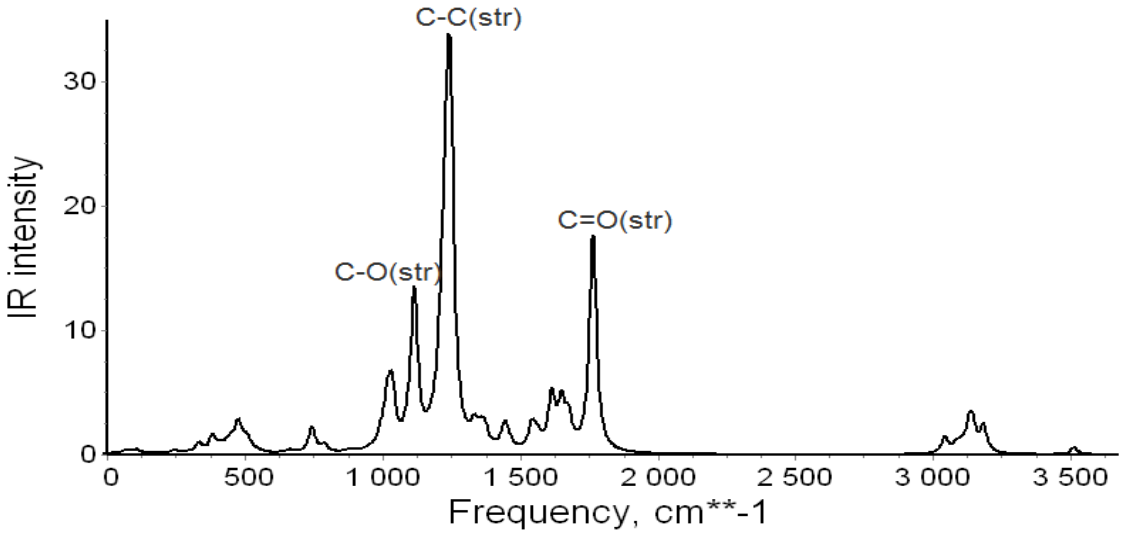

Figure 8: IR spectrum of crocetin.

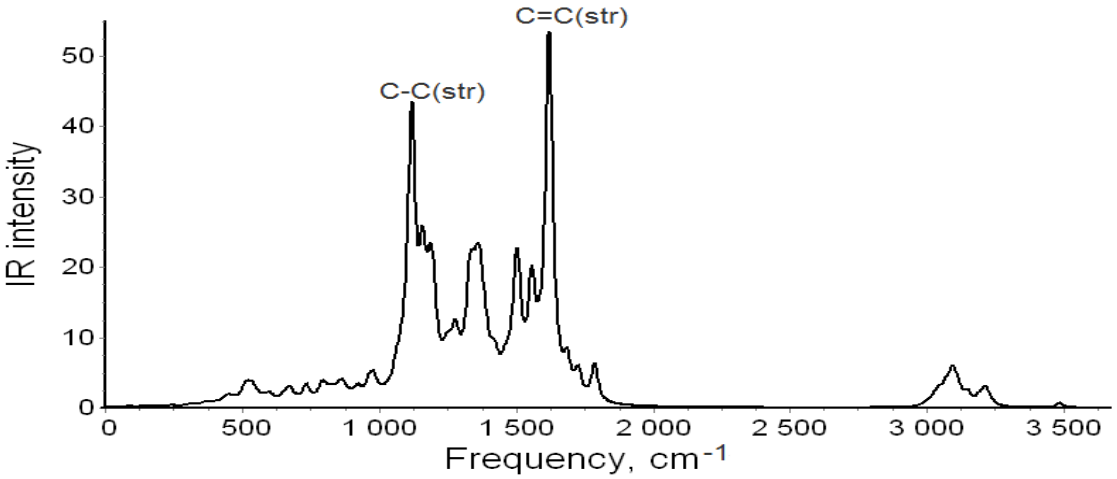

Figure 9: IR spectrum of indoline, D205.

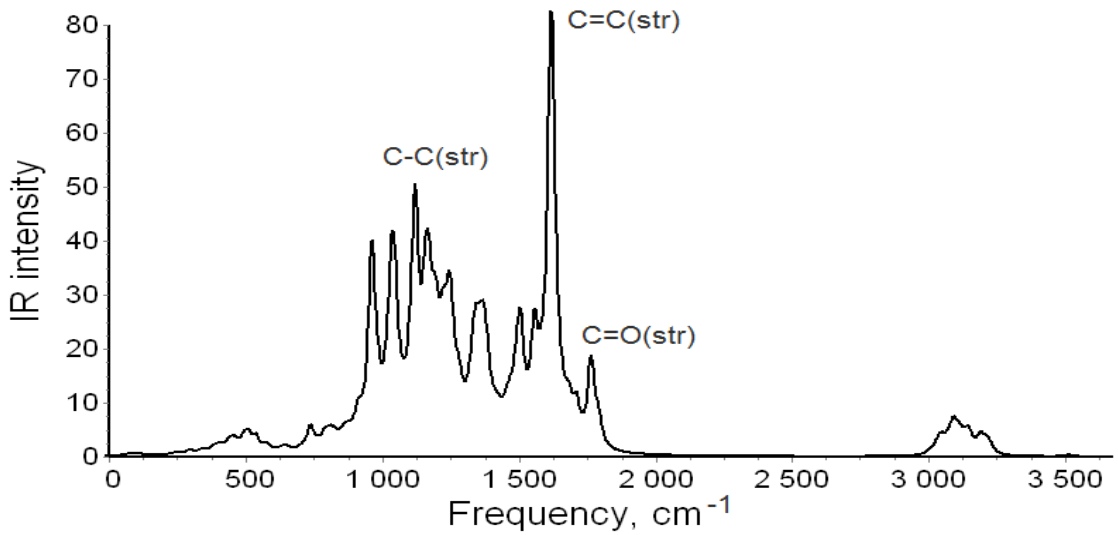

Figure 10: IR spectrum of the complex.

4.4 Vibrational spectra of the tocopherol and retinol molecules

Vibrational spectra of the species were calculated by DFT B3LYP5 method with 3-21G basis set. An absence of imaginary frequencies confirmed that the geometrical structures of the species corresponded to minima at the potential energy surfaces. The computed IR spectra are shown in Figs. 11 and 12. The most intensive modes in the spectra are assigned to the vibrations 1116cm^{-1} (C-C stretching), 1295cm^{-1} (C=C bending), 3051-3104cm^{-1} (C-H stretching), 3555cm^{-1} (O-H stretching) of the tocopherol molecule (Fig. 11) and 1007cm^{-1} (C-C stretching), 1269cm^{-1} (C-C bending, C-H bending), 1447cm^{-1} (2CH_3 bending), 1554cm^{-1} (C=C stretching), 3043 cm^{-1} (2CH_3 asymmetrical stretching), 3477cm^{-1} (O-H stretching) of the retinol molecule (Fig. 12).

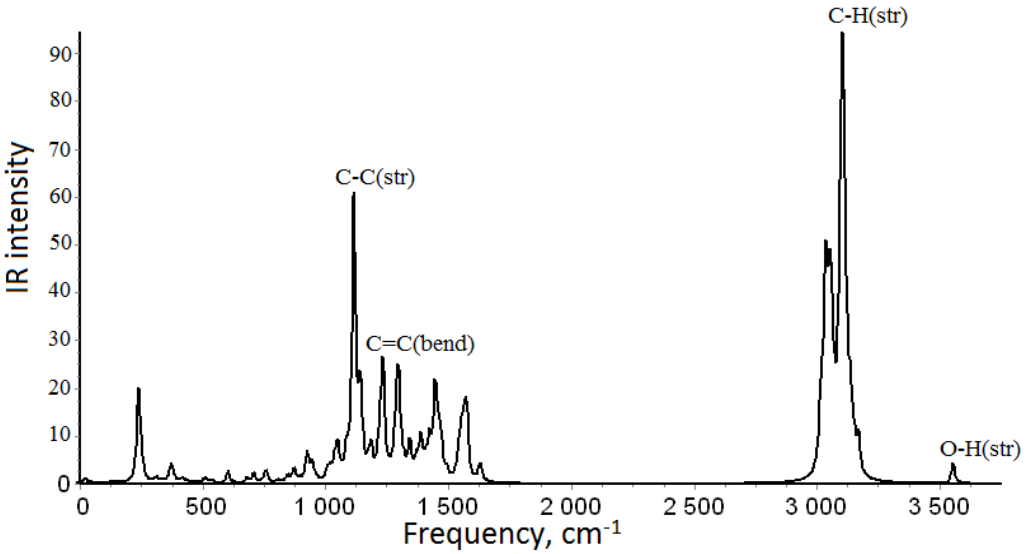

Figure 11: IR spectrum of tocopherol.

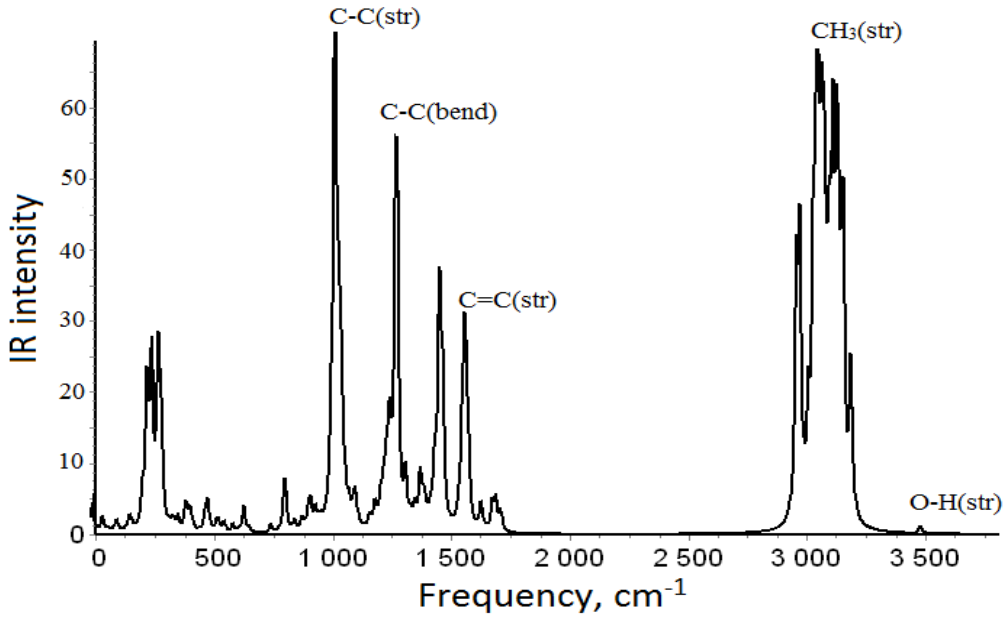

Figure 12: IR spectrum of retinol.

4.5 Electronic spectra of the species

For the two molecules under study, crocetin and indoline, as well as the complex designed the electronic spectra was computed for vacuum and for chloroform solution. The vertical excitation energies (E_{ex}), wavelengths (λ), oscillator strengths (f) and electronic configurations of the transitions are listed in Table 4. The singlet–singlet ($S_0 \rightarrow S_{ex}$) excitations with nonzero oscillator strengths ($f > 0.001$) were taken into account.

In spectra of all species the bands of maximum wavelengths are seen in visible region. For the crocetin and indoline molecules, the excitations from the ground to first excited state are of the highest oscillator strength and attributed to the HOMO-LUMO (H→L) transitions while for the complex the more probable transitions are to the second and third excited states and assigned mostly to H→L+1 and H–1→L.

For two other natural dyes, tocopherol and retinol, the electronic spectra were computed for vacuum and for ethanol solution. The vertical excitation energies (E_{ex}), wavelengths (λ), oscillator strengths (f) and electronic configurations of the transitions are listed in Table 5. The excitations of 10 states were considered in each case. The singlet–singlet ($S_0 \rightarrow S_{ex}$) excitations with nonzero oscillator strengths ($f > 0.001$) were taken into account.

In the spectra of both molecules, the bands of maximum wavelengths are seen in ultraviolet region. For the tocopherol the excitations H–1→L, λ = 195 nm, is of the highest oscillator strength. For the retinol molecule the most probable transition is to the first excited state which corresponds to maximum wavelength, λ = 358 nm, is attributed to the HOMO-LUMO (H→L) transition.

Table 4: Electronic spectra of crocetin, indoline D205 and complex molecules (TD-DFT B3LYP5/6-31G).

No of excited state	E_{ex}, eV	λ, nm	f	Electronic transition configuration
Crocetin, vacuum				
1	2.53	490	1.882	H→L, 88→89
3	3.82	325	0.050	H–1→L, 87→89
5	3.87	321	0.021	H–3→L, 85→89
6	3.93	316	0.053	H→L+2, 88→91
7	4.19	296	0.078	H–1→L+1, 87→90
9	4.80	258	0.040	H–3→L+1, 85→90
Crocetin, chloroform				
1	2.46	504	1.871	H→L, 88→89
3	3.77	329	0.066	H–1→L, 87→89
4	3.88	320	0.100	H→L+2, 88→91
5	4.10	302	0.064	H–1→L+1, 87→90
9	4.80	259	0.491	H–2→L, 86→89
Indoline D205, vacuum				
1	2.37	520	1.042	H→L, 218→219
3	2.99	414	0.567	H–1→L, 217→219
4	3.16	392	0.212	H→L+1, 218→220
5	3.39	366	0.227	H–3→L, 215→219
6	3.58	347	0.092	H→L+2, 218→221
8	3.82	325	0.068	H–1→L+1, 217→220
9	3.95	314	0.021	H-7→L, 211→219
10	3.98	311	0.023	H–4→L, 214→219
Indoline D205, chloroform				
1	2.16	574	0.807	H→L, 218 →219
2	2.84	436	0.582	H–1→L, 217→219
3	2.95	421	0.355	H→L+1, 218→220
5	3.34	371	0.126	H–2→L, 216→219
6	3.53	351	0.343	H→L+2, 218 →221
7	3.69	336	0.030	H–1→L+1, 217→220
10	3.83	324	0.017	H-5→L, 213→219
Complex, vacuum				
1	1.99	624	0.002	H→L, 301 →302
2	2.33	531	1.666	H→L+1, 301 →303
3	2.44	509	1.741	H–1→L, 300 →302
5	2.59	479	0.001	H–2→L, 299 →302
6	2.85	435	0.003	H–3→L+1,298 →303
Complex, chloroform				
1	2.04	606	0.002	H→L, 301 →302
2	2.13	583	1.051	H→L+1, 301 →303
3	2.16	574	0.013	H–1→L+1, 300→303
4	2.32	533	2.017	H–1→L, 300 →302

Table 5: Electronic spectra of tocopherol, and retinol molecules (TD-DFT B3LYP5/6-31G).

No. of excited state	E_{ex}, eV	λ, nm	f	Electronic transition configuration
Tocopherol, vacuum (B3LYP5/6-31G(d,p))				
1	4.69	265	0.064	H→L,(120→121)
2	5.55	224	0.031	H→L+1, 120→122
4	6.26	198	0.111	H→L+3, 120→124
5	6.36	195	0.598	H-1→L, 119→121
6	6.52	190	0.359	H-1→L+1, 119→122
7	6.78	183	0.013	H→L+5, 120→126
8	6.82	182	0.015	H-1→L+2, 119→123
10	7.07	175	0.054	H-2→L,118→121
Tocopherol, ethanol (B3LYP5/6-31G(d,p))				
1	4.71	263	0.061	H→L, 120→121
2	5.56	223	0.039	H→L+1, 120→122
4	6.37	195	0.653	H-1→L, 119→121
5	6.48	191	0.378	H-1→L+1, 119→122
6	6.69	185	0.027	H→L+3, 120→124
7	7.00	177	0.099	H-3→L, 117→121
Retinol, vacuum (B3LYP5/6-31G(d,p))				
1	3.47	358	1.163	H→L,79→80
2	4.14	300	0.013	H-1→L,78→80
3	4.69	264	0.042	H→L+1,79→81
5	5.46	227	0.013	H-3→L,76→80
6	5.57	223	0.011	H-4→L,75→80
7	5.64	220	0.036	H-1→L+1,78→81
8	5.87	211	0.034	H-5→L,74→80
9	5.95	208	0.060	H-5→L,74→80
Retinol, ethanol (B3LYP5/6-31G(d,p))				
1	3.46	359	1.139	H→L,79→80
2	4.11	302	0.043	H-1→L,78→80
3	4.67	265	0.036	H→L+1,79→81
5	5.44	228	0.019	H-3→L,76→80
7	5.62	221	0.040	H-1→L+1,78→81
9	5.98	207	0.082	H→L+2,79→82

The theoretical electronic spectra of the molecules are compared to our experimental UV-vis spectra of the dyes in chloroform/ethanol solutions (Figs. 13-17). The theoretical results for UV-vis spectra of crocetin (Figs. 13a, b) indicate a slight red shift of the maximum wavelength from vacuum (λ = 490 nm) to chloroform solution (λ = 504 nm). In experimental spectrum of crocetin (Fig. 13c), the broad bands are observed with maxima at 286, 412, 436, and 462 nm, the latter two are overlapping resulting in highest intensity bands. This experimental spectrum does not contradict much to the theoretical results (Figs. 13 a, b) and in a good agreement with data obtained in (Harbourne, 1984) where the peaks at 415, 433 and 462 nm were observed in the visible range of the spectrum for crocetin in chloroform.

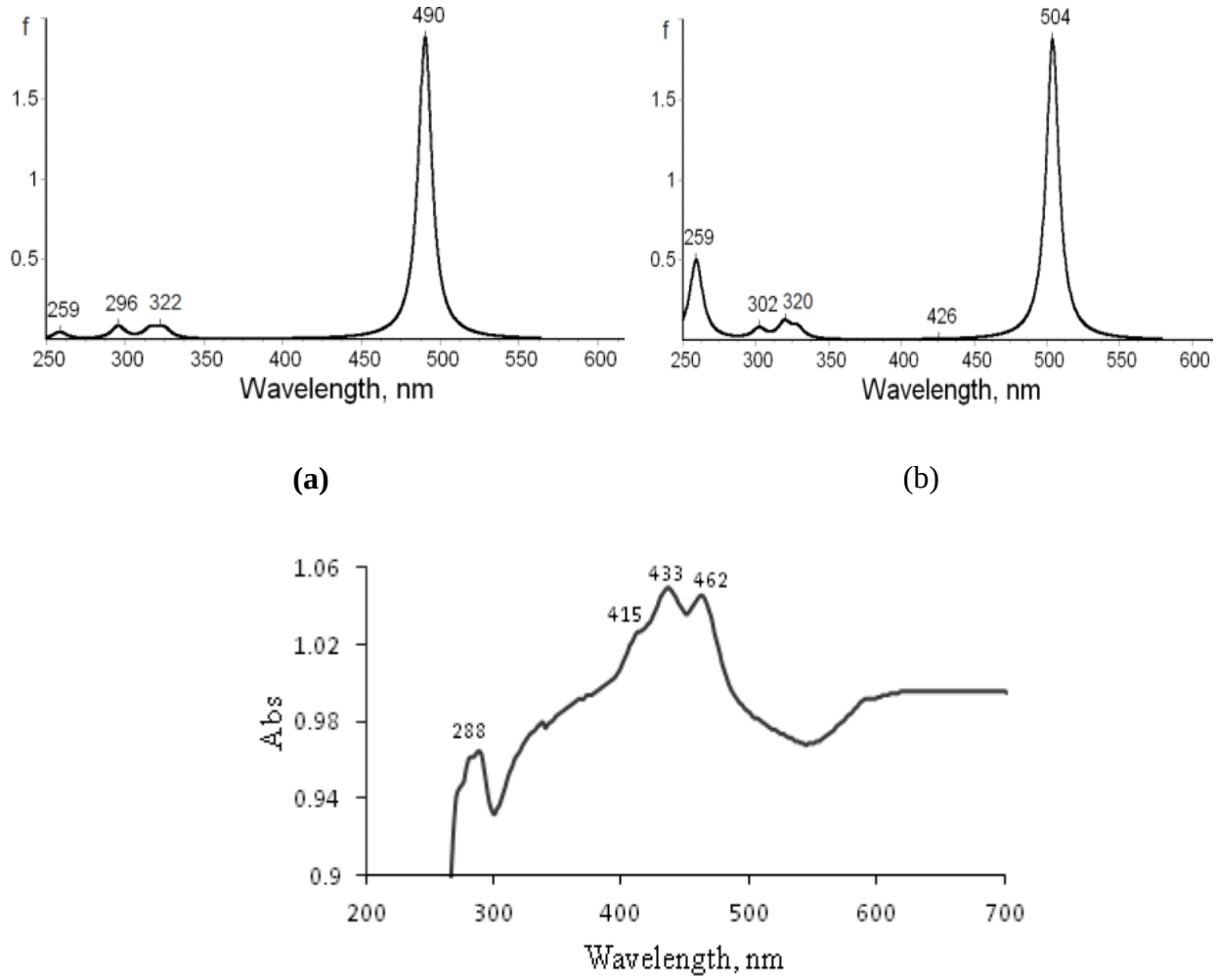

Figure 13: UV-vis spectrum of crocetin: (a) computed for vacuum; (b) computed for chloroform solution; (c) experimental for chloroform solution.

In the theoretical UV-vis spectra of indoline (Figs. 14a, b), the peaks of high intensity are at 415 and 523 nm (vacuum) and at 435 and 577 nm (chloroform), thus the red shift is seen from vacuum to solution. In the experimental spectrum in chloroform (Fig. 14c), the most intensive band lies in the UV region with three maxima at 288, 338, 370 nm and broad band of low intensity is observed in the range 500-600 nm. The appearance of the theoretical and experimental spectra looks different regarding intensities of the peaks, still an accordance may be noted between wavelengths in spectra computed for indoline dye (523, 577 nm) and measured experimentally (~550-560 nm). Our experimental result agrees well with the value λ = 554 nm observed earlier in spectrum of indoline dye D205 in chloroform solution (Higashijima *et al.*, 2011).

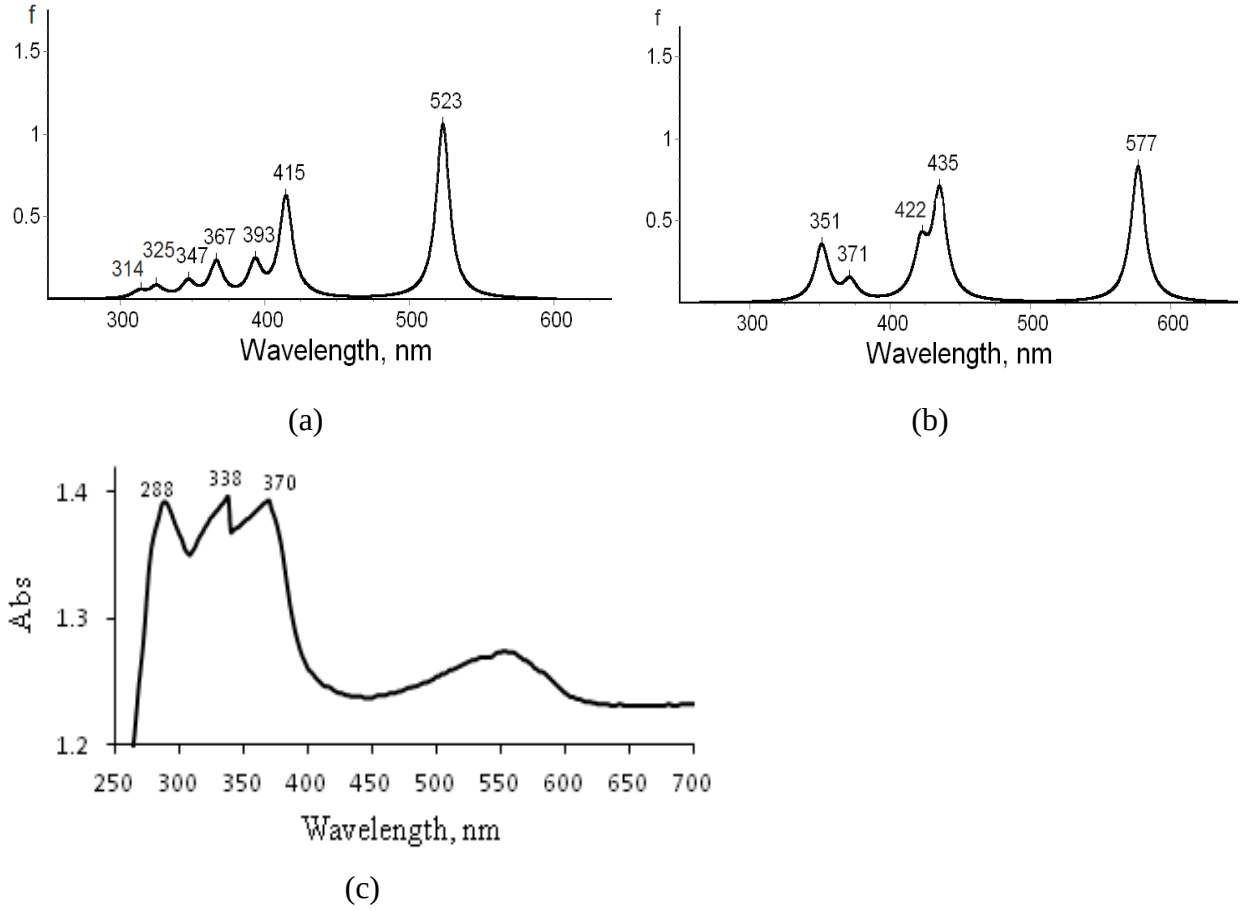

Figure 14: UV-vis spectrum of indoline: (a) computed for vacuum; (b) computed for chloroform solution; (c) experimental for chloroform solution**.**

The computed UV-vis spectrum of the complex contains two intensive peaks (Figs. 15 a, b). Peaks at 531 nm (vacuum) and 583 nm (chloroform) correspond to those in spectra of the indoline D205 molecule: 523 and 577 nm for vacuum and chloroform, respectively. For the complex molecule, the peak at 509 nm (vacuum) or 533 nm (chloroform) does not correspond to any transition neither for crocetin nor indoline. One can suggest that this peak may relate to the new formed bond C19-O3-C23 in the complex molecule. That means that the combination of two dyes allows widening of the light adsorption in visible range and thus improving the sensitizing ability of the dye.

In the experimental spectrum of the mixture (Fig. 15c), four maxima were identified, three in visible region (434, 460 and ~550 nm) and one in ultraviolet (290 nm). Two peaks among them resemble those in spectrum of individual crocetin, 436 and 462 nm (Fig. 13c) while the other two peaks correspond to those in spectrum of individual indoline dye D205, 288 and ~554 nm (Fig. 14c). If compare the theoretical spectrum of the complex molecule and experimental for the mixture, one can see that two sharp peaks in the former look like merged

into one broaden band in the latter. However no strong evidence of chemical interaction between individual dyes in solution is noticed. This observation is in accordance with the conclusion based on thermodynamic approach (Table 3) that the reaction (1) of complex formation is not thermodynamically favorable being endothermic and non-spontaneous.

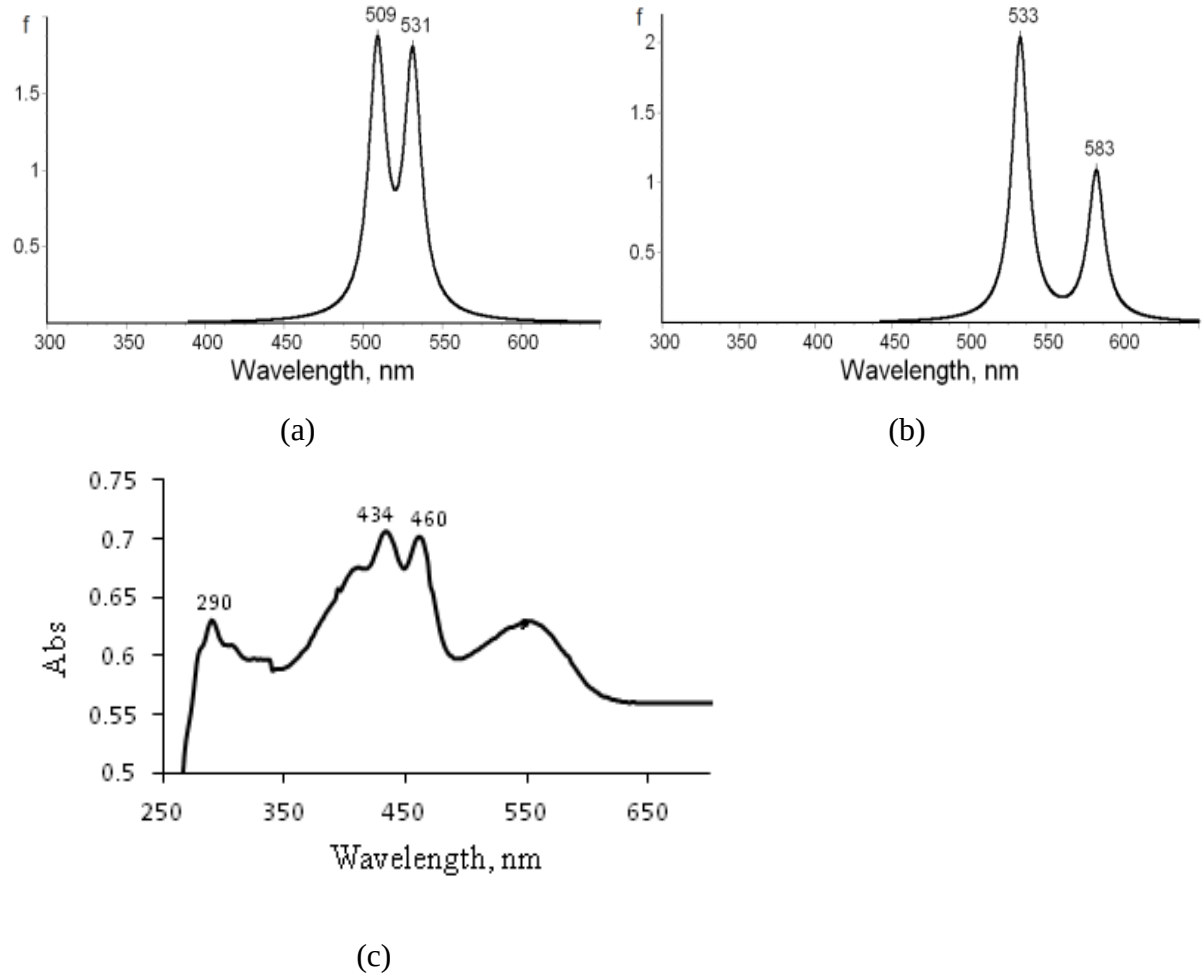

Figure 15: UV-vis spectra of the combination of two dyes, crocetin and indoline D205: (a) computed for the complex molecule in vacuum; (b) computed for the complex molecule in chloroform solution; (c) measured experimentally for the mixture of two dyes in chloroform solution.

In the theoretical UV-vis spectra of tocopherol (Figs. 16a, b), the peaks of high intensity are at 195 nm (vacuum) and 195 nm (ethanol) and a broad band of low intensity is observed at a region around 170-190 nm, thus there is no change in absorption spectrum is seen from vacuum to solution. The only difference is seen on the maximum wavelength. The theoretical results for UV-vis spectra of tocopherol indicate the maximum wavelength λ = 265 nm for vacuum and λ =263 nm for ethanol solution. On the other hand in experimental spectrum (Fig. 16c) the maximum wavelength for tocopherol in ethanol solution was observed at λ =

282 nm. These results agree well between each other and with data in literature,λ = 270 nm (Bakhouche *et al.*, 2015). It can be concluded that there is a good agreement between experimental, theoretical results and literature data as there is no big difference between them (282 nm, 264 nm and 270 nm, respectively) although results show no absorption in the visible region.

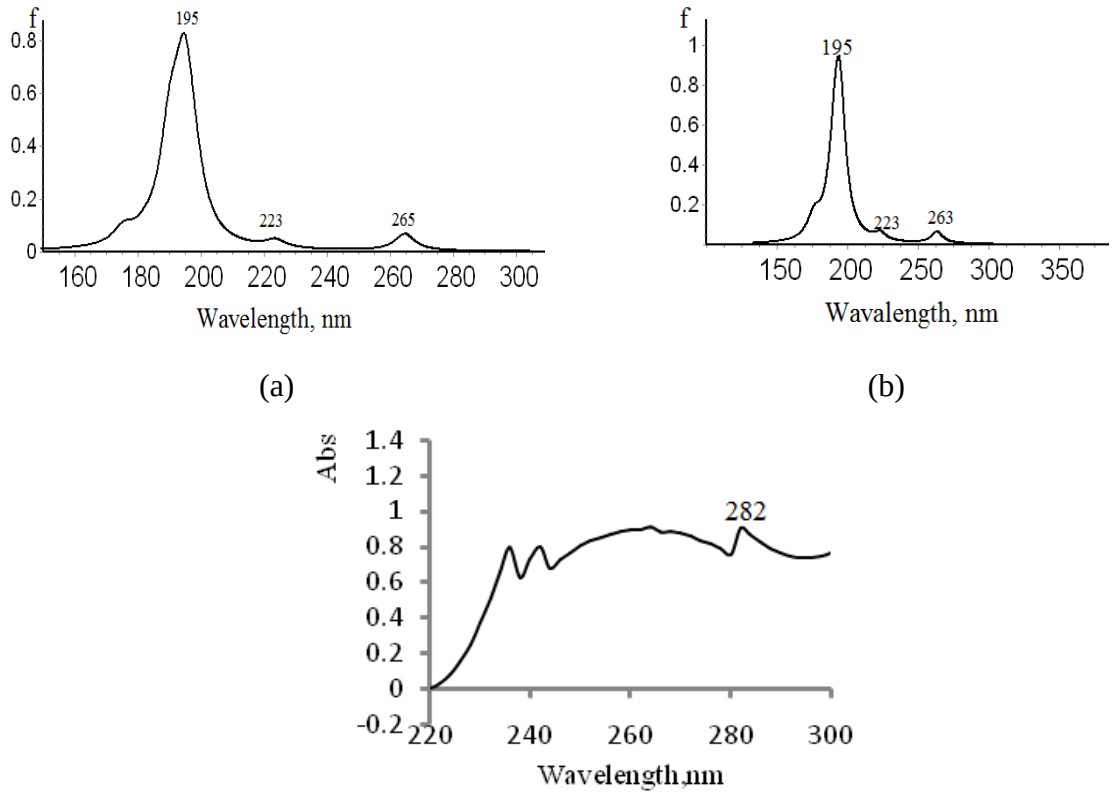

(a) (b)

(c)

Figure 16: UV-vis spectrum of tocopherol: (a) computed for vacuum; (b) computed for ethanol solution; (c) experimental for ethanol solution.

In the theoretical UV-vis spectra of retinol (Figs. 17a, b), the peak of high intensity are at 358 nm (vacuum) and 359 nm (ethanol) and a broad band of low intensity is observed at a region around 200-300 nm, thus the change in absorption range is seen from vacuum to solution to a small extent. The theoretical results for UV-vis spectra of retinol indicate the maximum wavelength 358 nm in vacuum and 359 nm in ethanol solution. On the other hand in experimental spectrum (Fig. 17c) the maximum wavelength for retinol in ethanol solution was observed at λ = 330 nm. It can be concluded that our experimental finding shows a good agreement with the datum available in literature, ~330 nm (Fugate and Song, 1980), but slightly differs from our computational results, 358 and 359 nm for vacuum and solution, respectively.

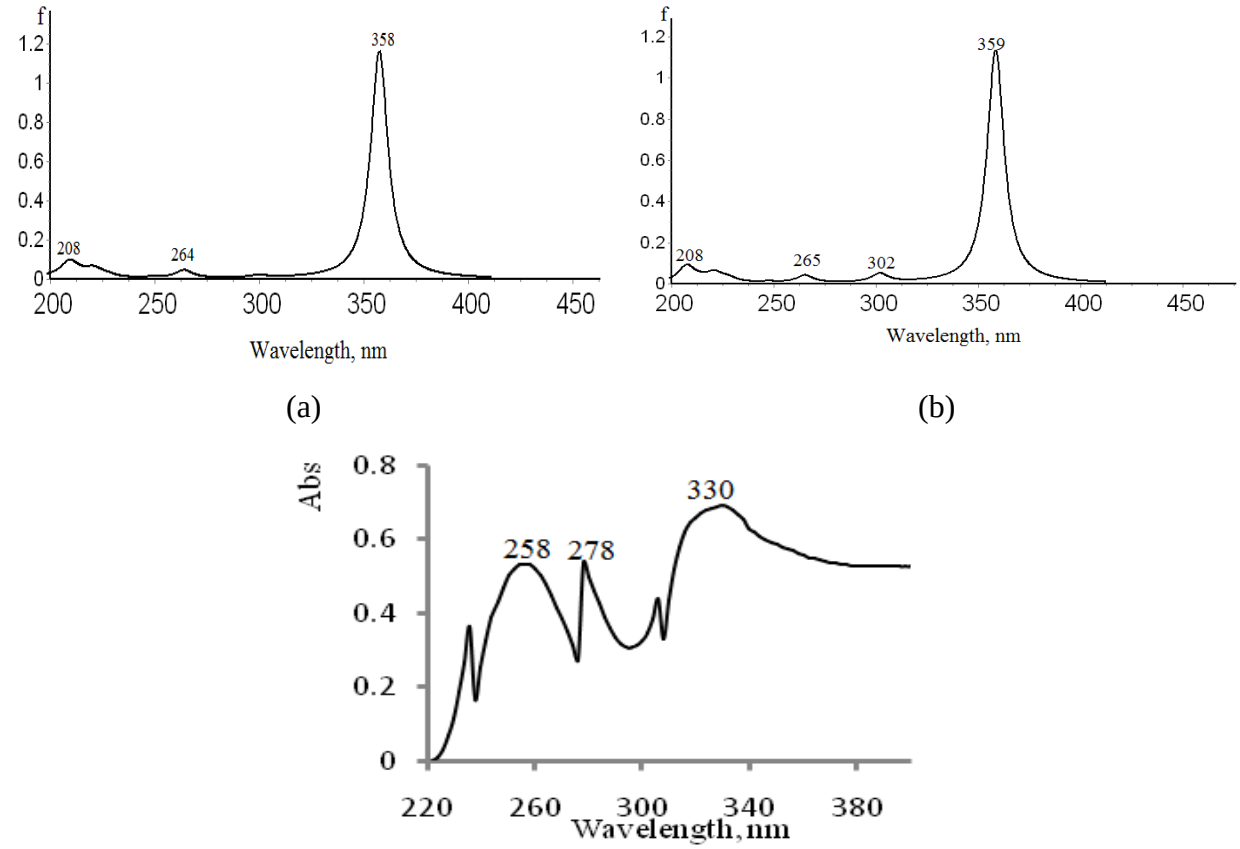

Figure 17: UV-vis spectrum of retinol: (a) computed for vacuum; (b) computed for ethanol solution; (c) experimental for ethanol solution.

4.6 Analysis of frontier molecular orbitals and energy levels alignment

Useful information about electronic structure of molecules and mechanisms of chemical reactions can be revealed from analysis of molecular orbitals (Le Bahers *et al.*, 2009b; Lin *et al.*, 2013). For the crocetin and indoline D205 molecules in vacuum, the frontier orbitals isosurfaces and energies are shown in Figs. 18 and 19. The number of occupied orbitals is 88 for crocetin and 218 for indoline molecules. From the shape of the orbitals, it is seen that in crocetin, both HOMO and LUMO are delocalized and electron density is distributed along the carbon chain. In indoline, the frontier orbitals are more localized; HOMO is located mostly on the diphenylethenyl part and on the indoline ring and LUMO on the rhodanine rings. In the electronic spectra of both molecules, the excitation $S_0 \rightarrow S_1$ is specified with high oscillator strengths (Table 4), and HOMO→LUMO transition contributes mostly to this first excited state transition.

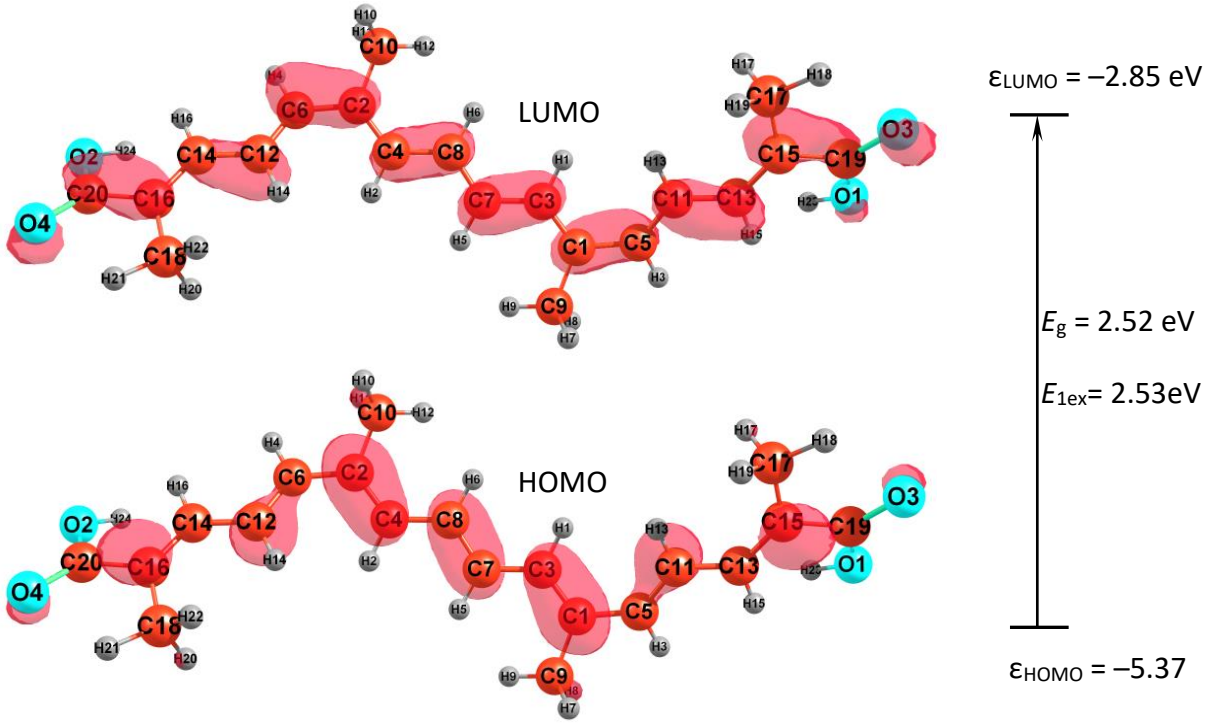

Figure 18: Frontier orbitals HOMO and LUMO in the crocetin molecule.

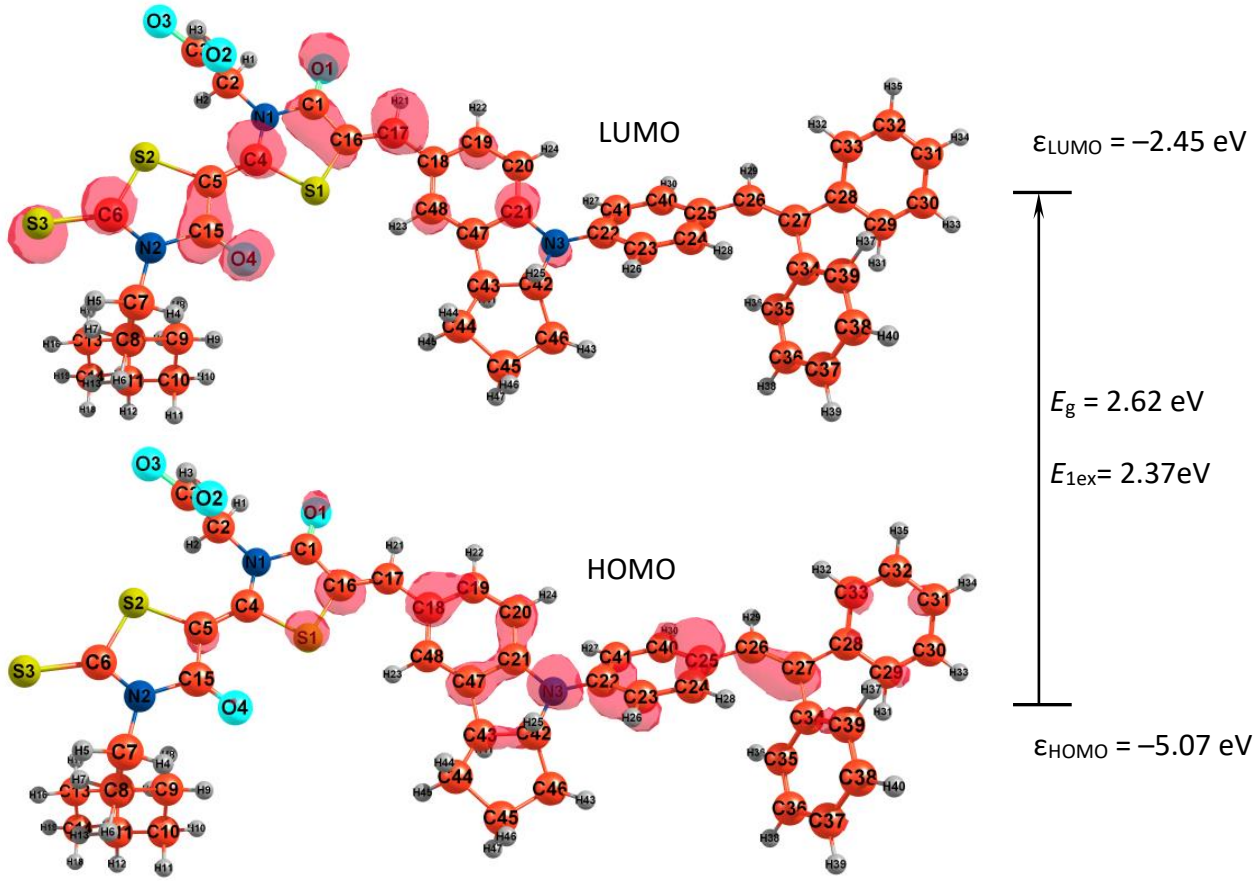

Figure 19: Frontier orbitals HOMO and LUMO in the indoline D205 molecule.

The frontier and adjacent orbitals (HOMO, LUMO, H–1, and L+1) of the complex molecule in vacuum are displayed in Fig. 20. The number of occupied orbitals is 301. The HOMO is located on the indoline part while LUMO is at the crocetin site (Fig. 20a). This implies that when an electron transfers from the HOMO to LUMO, the electron density significantly decreases in the electron-donating indoline moiety, accompanied by increase in that of the electron-accepting crocetin site. Nevertheless, according to the results on oscillator strengths (Table 4), the most probable transitions are not HOMO→LUMO, but H→L+1 and H–1→L. As is observed in Fig. 20b, the H–1 MO is located on the crocetin part of the complex, and L+1 MO on the indoline part. It means that the protruded picks of the electronic spectrum (Fig. 15a) is attributed to the transitions within either crocetin or indoline sites in the complex molecule.

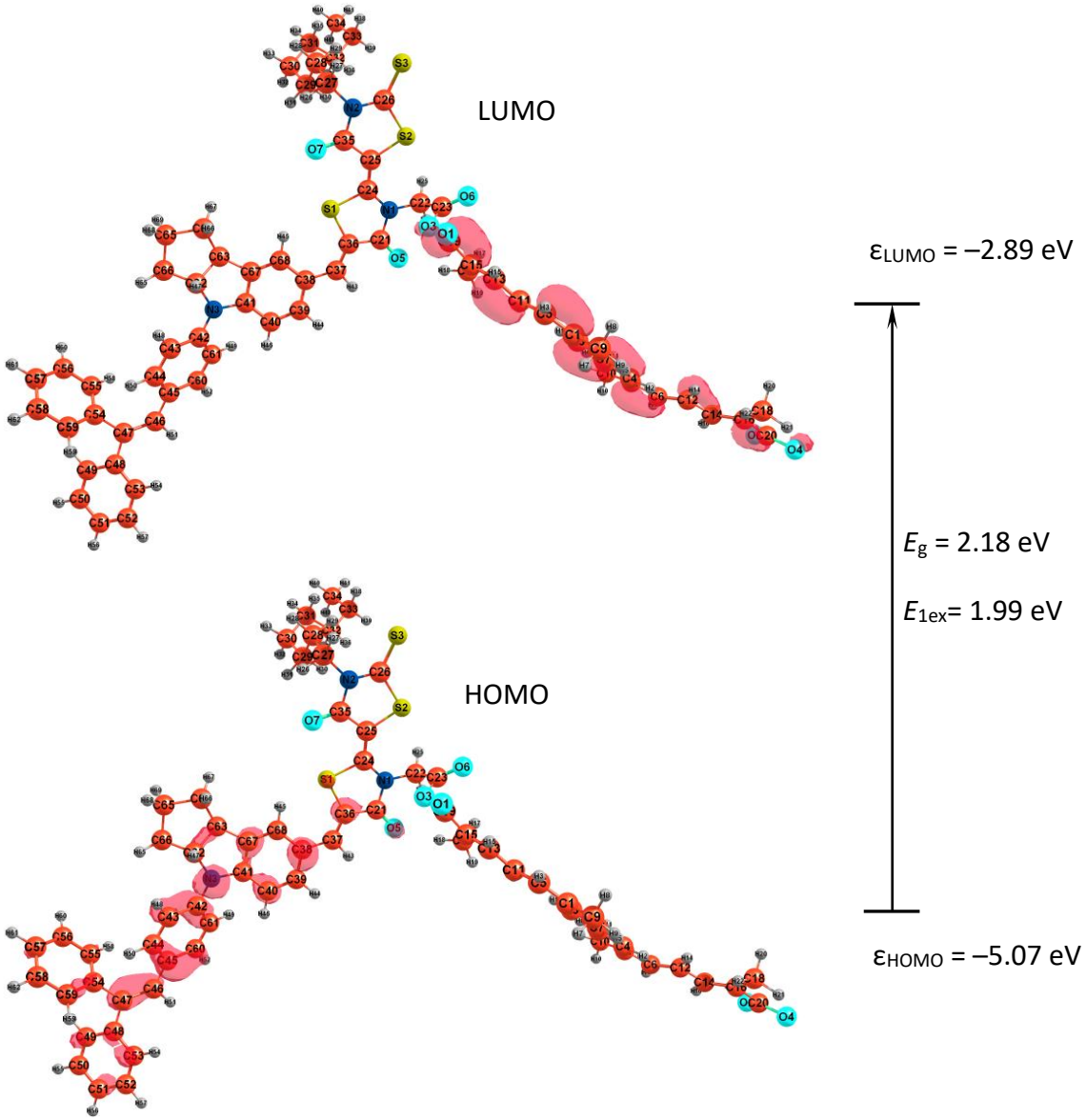

(a)

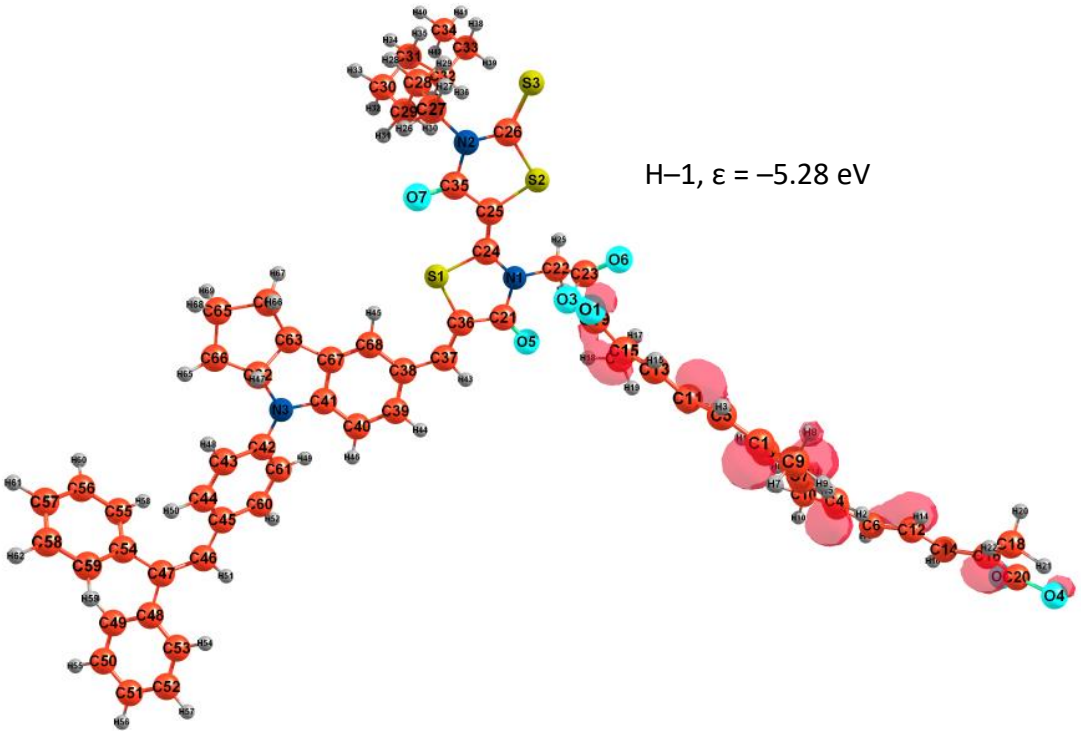

(b)

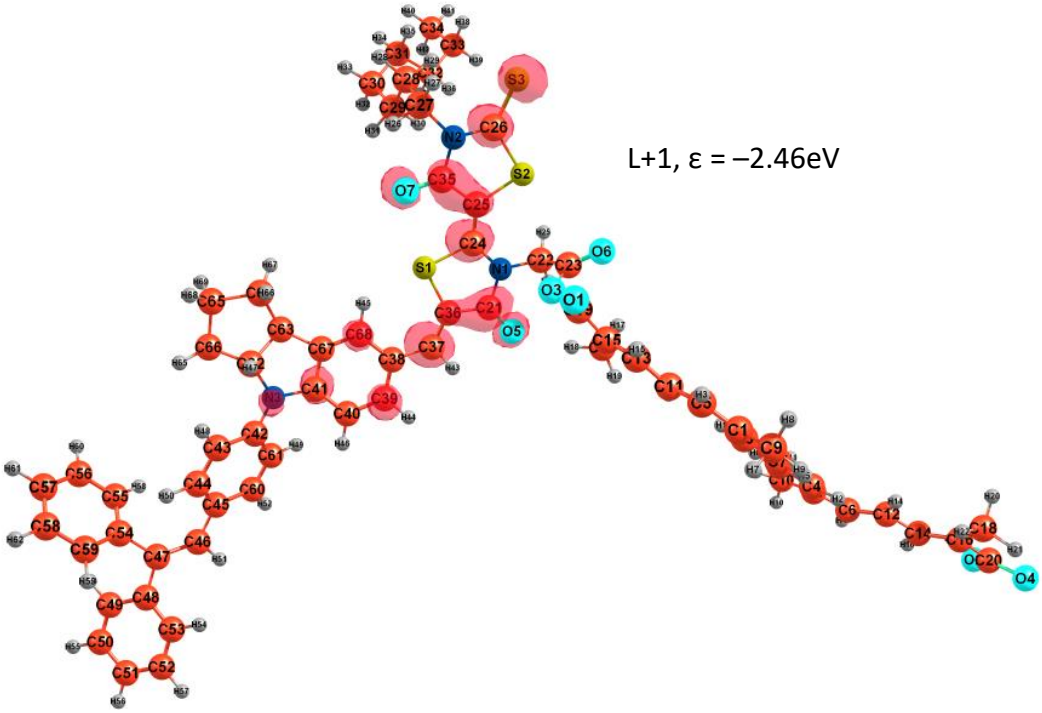

(c)

Figure 20: Frontier and adjacent MOs in the complex molecule: `
(a) HOMO and LUMO; (b)H–1; (c) L+1.

For the tocopherol and retinol molecules, the frontier orbitals isosurfaces and energies are shown in Figs. 21 and 22. The number of occupied orbitals is 120 for tocopherol and 79 for retinol molecules. From the shape of the orbitals, it is seen that in tocopherol, both HOMO and LUMO are delocalized and electron density is distributed along the carbon chain as well as in retinol molecule. In the electronic spectra of tocopherol molecule, the transition HOMO→LUMO is not of high probability. For retinol the excitation $S_0 \rightarrow S_1$ is specified with high oscillator strengths (Table 5), and HOMO→LUMO transition contributes mostly to this excitation.

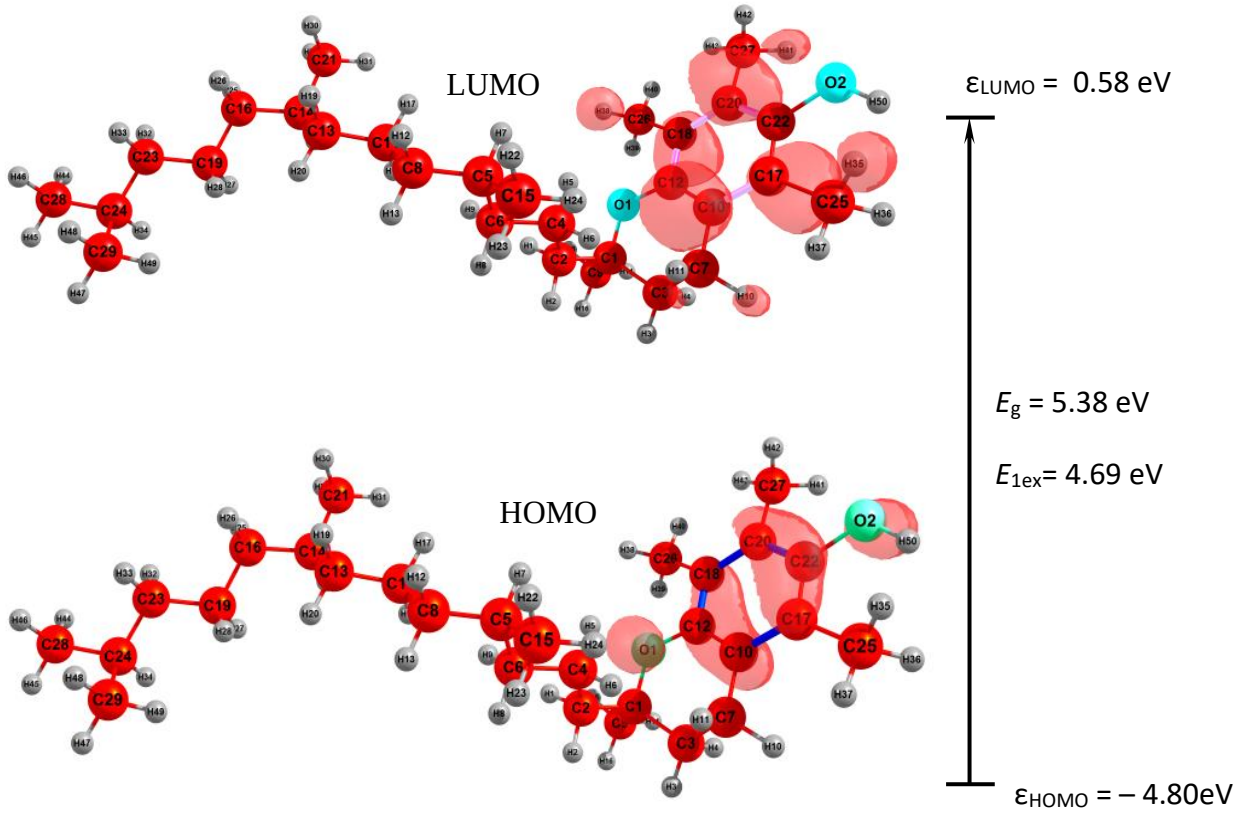

Figure 21: Frontier orbitals HOMO and LUMO in the tocopherolmolecule.

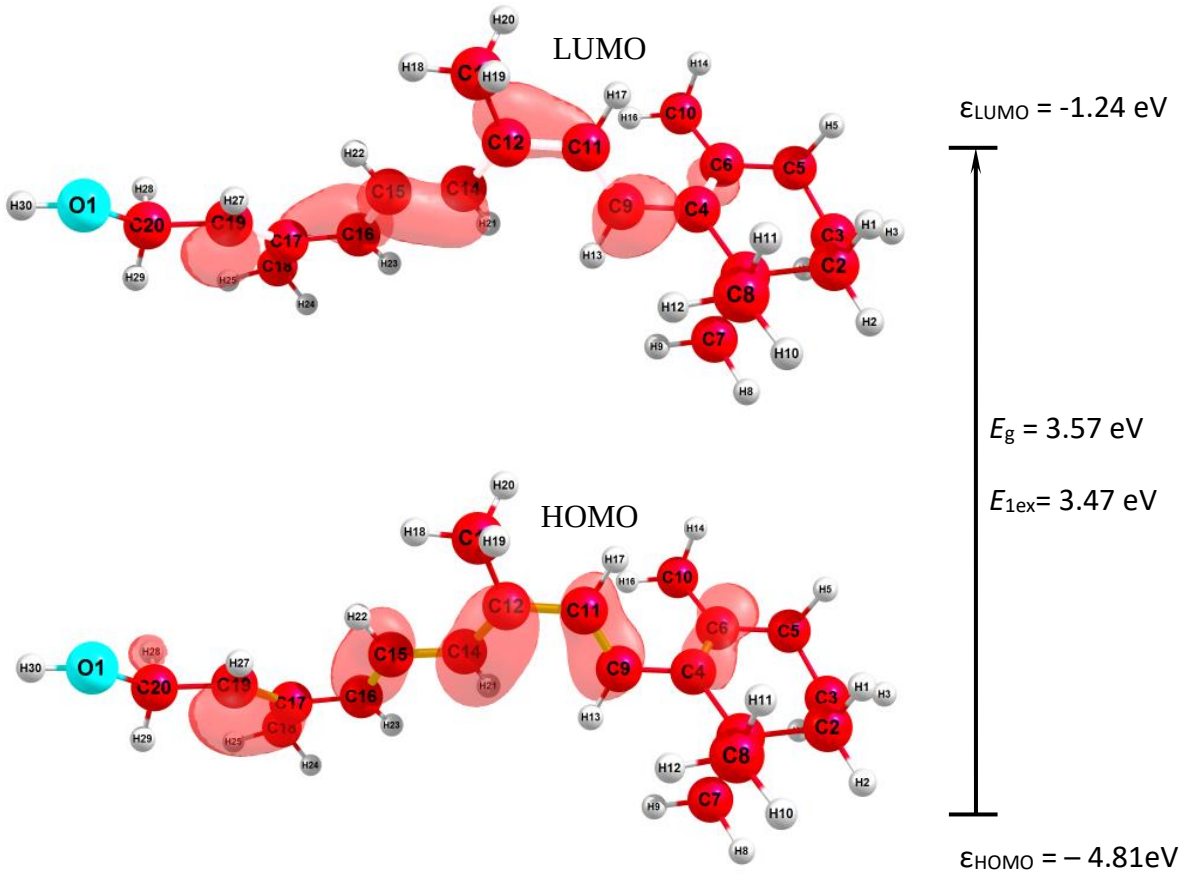

Figure 21: Frontier orbitals HOMO and LUMO in the retinol molecule.

A proper energy level alignment between a dye, semiconductor and electrolyte is a fundamental requirement for a DSSC. The simplest way to consider this alignment is drawing the frontier MOs energy levels together with valence and conduction bands of a semiconductor. However more strict approach is to implement the excitation energies E_{ex} obtained by TD-DFT and calculate the excited state potentials *ESP* (Oprea *et al.*, 2011). In our work, the values of *ESP* were found as sums of the ground state occupied MOs energies and respective excitation energies E_{ex}, $ESP = \varepsilon(\text{HOMO}) + E_{ex}$. The calculated energies of frontier and adjacent molecular orbitals ε(MO), excitation energies E_{ex}, energy differences between MOs E_g, and excited state potentials *ESP* are presented in Table 6. The values of E_{ex} and E_g correspond to transitions between the orbitals shown in respective column.

Although an analysis of the frontier orbitals is illustrative and useful for understanding of electron transfer mechanism, the values of excitation energies allow entire electronic spectra modeling and correct representation of electron transitions. As is seen, the values of energy gap between HOMO and LUMO (E_g) coincide with the first excitation energy (E_{ex}) for

crocetin molecule; this is valid for vacuum and chloroform solution. For indoline and complex molecules, these quantities differ, the values of E_g is bigger, as a rule, the difference approaches 0.5 eV. These differences result in lowering the *ESPs* compared to respective unoccupied orbitals.

Table 6: The energies of molecular orbitals ε(MO), excitation energies E_{ex}, energy differences between MOs E_g, and excited state potentials *ESP*; all values in eV.

MO	–ε(MO)	Transition	E_{ex}	E_g	–*ESP*
		Crocetin, vacuum			
88, H	5.37	H→L	2.53	2.52	2.84
89, L	2.85				
		Crocetin, chloroform			
88, H	5.12	H→L	2.46	2.46	2.66
89, L	2.66				
		Indoline D205, vacuum			
218, H	5.07	H→L	2.37	2.62	2.70
219, L	2.45				
		Indoline D205, chloroform			
218, H	5.11	H→L	2.15	2.37	2.96
219, L	2.74				
		Complex, vacuum			
300, H–1	5.28	H→L	1.99	2.18	3.08
301, H	5.07	H→L+1	2.33	2.39	2.95
302, L	2.89	H–1→L	2.44	2.91	2.63
303, L+1	2.46				
		Complex, chloroform			
300, H–1	5.18	H→L	2.04	2.24	3.09
301, H	5.13	H→L+1	2.13	2.36	3.00
302, L	2.89	H–1→L	2.32	2.29	2.86
303, L+1	2.77				

The diagram in Fig. 23 shows the energy levels of HOMOs and *ESPs* of the molecules under study for chloroform solutions; the valence and conduction bands of the semiconductors TiO_2 (De Angelis *et al.*, 2008; Oprea *et al.*, 2011) and ZnO (Le Bahers *et al.*, 2009a), redox level of theI^-/I_3^- electrolyte (Peter, 2007; De Angelis *et al.*, 2008; Han *et al.*, 2015) are given for comparison. According to requirements, the HOMO and LUMO levels of a dye must match with the conduction-band-edge energy level of the semiconductor and the redox potential of electrolyte for an efficient charge separation and dye regeneration (Hara *et al.*, 2003); the HOMO level of the sensitizer has to be lower than the redox potential and the first excited state of the dye has to be slightly higher than the conduction band of the semiconductor (Hagfeldt and Graetzel, 1995; Liu, 2008). As is observed on the diagram, all three molecules meet the criteria for sensitizers: HOMO levels lie below the redox level of the electrolyte, and

the excited state potentials lie above or coincide with conduction bands of semiconductors. That is the injection of electrons from the dyes to the conduction bands of TiO_2 or ZnO can occur. For the complex it is expected even higher performance due to the energy levels better meet requirements for sensitizer as the complex possesses smaller excitation energies (2.04, 2.13 and 2.32 eV for the complex compared to 2.46 eV for crocetin and 2.15 eV for indoline). Moreover, the transitions, from H–1 to the first excited state and from HOMO to second excited state are of high probability to be involved in sensitizing semiconductor, and the two corresponding *ESP* levels (–2.86 and –3.00 eV) match well with the conduction band of ZnO (–2.96 eV).

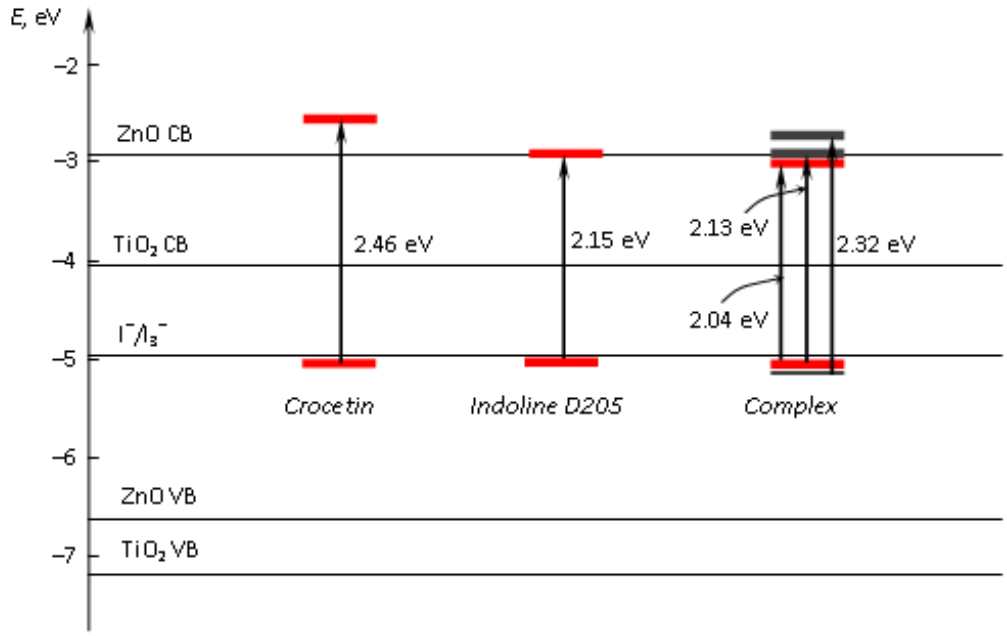

Figure 22: Energy level diagram of HOMOs and excited state potentials of crocetin, indoline D205 and complex molecules in chloroform.

CHAPTER FIVE

CONCLUSION AND RECOMMENDATIONS

5.1 Conclusion

The properties of the dye molecules, crocetin, indoline, tocopherol, and retinol, have been studied by DFT and TD-DFT methods. The equilibrium structures of the molecules, IR and electronic spectra were computed and analyzed. Experimental measurements of UV-vis spectra of the dyes' solutions were performed. The absorption bands in experimental UV-vis spectra of the individual dyes are reproduced adequately by theoretical TD-DFT computations.

Molecular design of a new solar cell sensitizer was attempted through the combination of two individual dyes, natural crocetin and synthetic indoline D205, aimed to improve optical properties of the materials. The thermodynamic approach indicated endothermicity and non-spontaneity of the direct joining of the components *via* C-O-C linkage. The combination of two dyes results in widening of light absorption visible range and better energy level alignment with the conduction band of semiconductor ZnO and redox level of the I^-/I_3^- electrolyte. Thus the complex molecule designed might possess enhanced power conversion efficiency compared to that of individual dyes.

5.2 Recommendations

(i) The synthesis of the designed complex composed of the crocetin and indoline D205 dyes and characterization of it with FT-IR and XRD technique.

(ii) The dye sensitized solar cells have to be fabricated *via* the use of the individual dyes and designed complex so as to study and compare the performance of the cells.This will enable to account for the effect of widening the absorption range on the efficiency of the cell.

(iii) Similar study on combination between tocopherol and retinol with indoline D205.

(iv) Studies on combination between crocetin and indoline dyes using advanced basis sets, e.g 6-311G (d, p), for the geometrical parameters optimization and computation of vibrational spectra of the dyes.

REFERENCES

Abdel-Latif, M. S., Abuiriban, M. B., El-Agez, T.M. and Taya, S. A. (2015). Dye-sensitized solar cells using dyes extracted from flowers, leaves, parks, and roots of three trees. *International Journal of Renewable Energy Research*. **5**(1): 294-298.

Akila, Y., Muthukumarasamy, N., Agilan, S., Mallick, T. K., Senthilarasu, S. and Velauthapillai, D. (2016). Enhanced performance of natural dye sensitised solar cells fabricated using rutile TIO_2 nanorods. *Optical Materials*. **58**(76-83.

Ambrosio, F., Martsinovich, N. and Troisi, A. (2012). What is the best anchoring group for a dye in a dye-sensitized solar cell? *The Journal of Physical Chemistry Letters*. **3**(11): 1531-1535.

Arjunan, T. and Senthil, T. (2013). Dye sensitised solar cells. *Materials Technology*. **28**(1-2): 9-14.

Bakhouche, K., Dhaouadi, Z., Jaidane, N. and Hammoutène, D. (2015). Comparative antioxidant potency and solvent polarity effects on HAT mechanisms of tocopherols. *Computational and Theoretical Chemistry*. **1060**(58-65.

Bisquert, J. and Vikhrenko, V. S. (2004). Interpretation of the time constants measured by kinetic techniques in nanostructured semiconductor electrodes and dye-sensitized solar cells. *The Journal of Physical Chemistry* . **108**(7): 2313-2322.

Bode, B. M. and Gordon, M. (1998). MacMolPlt version 7.4.2, Journal of Molecular Graphics and Modelling.

Boschloo, G., Häggman, L. and Hagfeldt, A. (2006). Quantification of the effect of 4-tert-butylpyridine addition to I-/I3-redox electrolytes in dye-sensitized nanostructured TiO_2 solar cells. *The Journal of Physical Chemistry* . **110**(26): 13144-13150.

Calogero, G. and Di Marco, G. (2008). Red Sicilian orange and purple eggplant fruits as natural sensitizers for dye-sensitized solar cells. *Solar Energy Materials and Solar Cells*. **92**(11): 1341-1346.

Calogero, G., Di Marco, G., Cazzanti, S., Caramori, S., Argazzi, R., Di Carlo, A. and Bignozzi, C.A. (2010). Efficient dye-sensitized solar cells using red turnip and purple wild sicilian prickly pear fruits. *International Journal of Molecular Science*. **11**(1): 254-67.

Campbell, W. M., Burrell, A. K., Officer, D. L. and Jolley, K. W. (2004). Porphyrins as light harvesters in the dye-sensitised TiO_2 solar cell. *Coordination Chemistry Reviews*. **248**(13): 1363-1379.

Chang, H. and Lo, Y. J. (2010). Pomegranate leaves and mulberry fruit as natural sensitizers for dye-sensitized solar cells. *Solar Energy*. **84**(10): 1833-1837.

Chiba, Y., Islam, A., Watanabe, Y., Komiya, R., Koide, N. and Han, L. (2006). Dye-sensitized solar cells with conversion efficiency of 11.1%. *Japanese Journal of Applied Physics*. **45**(7L): L638.

Dai, Q. and Rabani, J. (2002). Photosensitization of nanocrystalline TiO_2 films by anthocyanin dyes. *Journal of Photochemistry and Photobiology*. **148**(1): 17-24.

De Angelis, F., Fantacci, S. and Selloni, A. (2008). Alignment of the dye's molecular levels with the TiO_2 band edges in dye-sensitized solar cells: a DFT–TDDFT study. *Nanotechnology*. **19**(42): 424002.

Dong, H., Zhou, X. and Jiang, C. (2012). Molecular design and theoretical investigation on novel porphyrin derivatives for dye-sensitized solar cells. *Theoretical Chemistry Accounts*. **131**(2): 1102.

Fantacci, S., De Angelis, F., Wang, J., Bernhard, S. and Selloni, A. (2004). A Combined Computational and Experimental Study of Polynuclear Ru− TPPZ Complexes: Insight into the Electronic and Optical Properties of Coordination Polymers. *Journal of the American Chemical Society*. **126**(31): 9715-9723.

Fugate, R. D. and Song, P. (1980). Spectroscopic characterization of β-lactoglobulin-retinol complex. *Biochimica et Biophysica Acta (BBA)-Protein Structure*. **625**(1): 28-42.

Giribabu, L., Kanaparthi, R. K. and Velkannan, V. (2012). Molecular engineering of sensitizers for dye-sensitized solar cell applications. *The Chemical Record*. **12**(3): 306-328.

Gómez-Ortíz, N., Vázquez-Maldonado, I., Pérez-Espadas, A., Mena-Rejón, G., Azamar-Barrios, J. and Oskam, G. (2010). Dye-sensitized solar cells with natural dyes extracted from achiote seeds. *Solar Energy Materials and Solar Cells*. **94**(1): 40-44.

Granovsky, A. A. 2016. *Firefly version 8.2.0 www.http://classic.chem.msu.su/gran/firefly /index.html.*

Guillemoles, J. F., Barone, V., Joubert, L. and Adamo, C. (2002). A theoretical investigation of the ground and excited states of selected Ru and Os polypyridyl molecular dyes. *The Journal of Physical Chemistry A*. **106**(46): 11354-11360.

Hagfeldt, A., Boschloo, G., Sun, L., Kloo, L. and Pettersson, H. (2010). Dye-sensitized solar cells. *Chemical Reviews*. **110**(11): 6595-6663.

Hagfeldt, A. and Graetzel, M. (1995). Light-induced redox reactions in nanocrystalline systems. *Chemical Reviews*. **95**(1): 49-68.

Hamilton, J. (1977). The theory of the photographic process. *by TH James, Macmillan, New York*: 133.

Han, M. W., Ekanayake, P., Ming, L. C. and Yoong, V. N. (2015). DFT/TD-DFT Studies on the Lawsone (Henna) as a Photosensitizer for Dye-Sensitized Solar Cells. *Applied Mechanics and Materials*. **789-790**(56-60.

Hao, S., Wu, J., Huang, Y. and Lin, J. (2006). Natural dyes as photosensitizers for dye-sensitized solar cell. *Solar Energy*. **80**(2): 209-214.

Hara, K., Sato, T., Katoh, R., Furube, A., Ohga, Y., Shinpo, A., Suga, S., Sayama, K., Sugihara, H. and Arakawa, H. (2003). Molecular design of coumarin dyes for efficient dye-sensitized solar cells. *The Journal of Physical Chemistry*. **107**(2): 597-606.

Harbourne, J. (1984). Phytochemical methods: A guide to modern techniques of plant analysis. *Ghapman and Hall, London*: 4-120.

Higashijima, S., Miura, H., Fujita, T., Kubota, Y., Funabiki, K., Yoshida, T. and Matsui, M. (2011). Highly efficient new indoline dye having strong electron-withdrawing group for zinc oxide dye-sensitized solar cell. *Tetrahedron*. **67**(34): 6289-6293.

Horiuchi, T., Miura, H., Sumioka, K. and Uchida, S. (2004). High efficiency of dye-sensitized solar cells based on metal-free indoline dyes. *Journal of the American Chemical Society*. **126**(39): 12218-12219.

Ito, S., Miura, H., Uchida, S., Takata, M., Sumioka, K., Liska, P., Comte, P., Pechy, P. and Gratzel, M. (2008). High-conversion-efficiency organic dye-sensitized solar cells with a novel indoline dye. *Chemical Communications (Camb)*41): 5194-6.

Jasim, K. E., Al-Dallal, S. and Hassan, A.M. (2011). Natural dye-sensitised photovoltaic cell based on nanoporous TiO_2. *International Journal of Nanoparticles*. **4**(4): 359-368.

Kalyanasundaram, K. (2010). Dye-sensitized solar cells. EPFL presspp.

Karki, I., Nakarmi, J., Mandal, P. and Chatterjee, S. (2013). Absorption Spectra of Natural Dyes and Their Effect on Efficiency of ZnO Based Dye-Sensitized Solar Cells. *Nepal Journal of Science and Technology*. **13**(1): 179-185.

Kay, A. and Graetzel, M. (1993). Photosensitization of titania solar cells with chlorophyll derivatives and related natural porphyrins. *The Journal of Physical Chemistry*. **97**(23): 6272-6277.

Khazraji, A. C., Hotchandani, S., Das, S. and Kamat, P. V. (1999). Controlling dye (Merocyanine-540) aggregation on nanostructured TiO2 films. An organized assembly approach for enhancing the efficiency of photosensitization. *The Journal of Physical Chemistry*. **103**(22): 4693-4700.

Kimpa, M. I., Momoh, M., Isah, K. U., Yahya, H. N. and Ndamitso, M. M. (2012). Photoelectric characterization of dye sensitized solar cells using natural dye from pawpaw leaf and flame tree flower as sensitizers. *Materials Sciences and Applications*. **3**(5): 281-286.

Kimura, M., Nomoto, H., Masaki, N. and Mori, S. (2012). Dye molecules for simple co-sensitization process: fabrication of mixed-dye-sensitized solar cells. *Angewandte International Edition Chemie*. **51**(18): 4371-4.

Kishimoto, S., Maoka, T., Sumitomo, K. and Ohmiya, A. (2005). Analysis of carotenoid composition in petals of calendula (Calendula officinalis L.). *Bioscience, Biotechnology, and Biochemistry*. **69**(11): 2122-2128.

Kuang, D., Uchida, S., Humphry-Baker, R., Zakeeruddin, S. M. and Grätzel, M. (2008). Organic Dye-Sensitized Ionic Liquid Based Solar Cells: Remarkable Enhancement in Performance through Molecular Design of Indoline Sensitizers. *Angewandte International Edition Chemie*. **120**(10): 1949-1953.

Kuang, D., Walter, P., Nüesch, F., Kim, S., Ko, J., Comte, P., Zakeeruddin, S.M., Nazeeruddin, M.K. and Grätzel, M. (2007). Co-sensitization of organic dyes for efficient ionic liquid electrolyte-based dye-sensitized solar cells. *Langmuir*. **23**(22): 10906-10909.

Ladomenou, K., Kitsopoulos, T., Sharma, G. and Coutsolelos, A. (2014). The importance of various anchoring groups attached on porphyrins as potential dyes for DSSC applications. *Royal Society of Chemistry*. **4**(41): 21379-21404.

Le Bahers, T., Pauporte, T., Scalmani, G., Adamo, C. and Ciofini, I. (2009a). A TD-DFT investigation of ground and excited state properties in indoline dyes used for dye-sensitized solar cells. *Physical Chemistry Chemical Physics*. **11**(47): 11276-84.

Le Bahers, T., Pauporté, T., Scalmani, G., Adamo, C. and Ciofini, I. (2009b). A TD-DFT investigation of ground and excited state properties in indoline dyes used for dye-sensitized solar cells. *Physical Chemistry Chemical Physics*. **11**(47): 11276-11284.

Lin, H., Zhu, S. G., Chen, P. Y., Li, K., Li, H. Z. and Peng, X. H. (2013). Dft investigation of a high energy density polynitro compound, 2, 2'-Bis (trinitromethyl)-5, 5'-azo-1, 2, 3, 4-tetrazole. *Central European Journal of Energetic Materials*. **10**(3): 325-338.

Liu, Z. (2008). Theoretical studies of natural pigments relevant to dye-sensitized solar cells. *Journal of Molecular Structure.* **862**(1): 44-48.

Matsui, M., Tanaka, N., Kubota, Y., Funabiki, K., Jin, J., Higashijima, S., Miura, H. and Manseki, K. (2016). Long-term stability of novel double rhodanine indoline dyes having one and two anchor carboxyl group (s) in dye-sensitized solar cells. *Royal Society of Chemistry*. **6**(39): 33111-33119.

Mphande, B. C. and Pogrebnoi, A. (2014). Impact of extraction methods upon light absorbance of natural organic dyes for dye sensitized solar cells application. *Journal of Energy and Natural Resources*. **3**(3): 38-45.

Narayan, M. R. (2012). Dye sensitized solar cells based on natural photosensitizers. *Renewable and Sustainable Energy Reviews*. **16**(1): 208-215.

Nazeeruddin, M. K., Kay, A., Rodicio, I., Humphry-Baker, R., Müller, E., Liska, P., Vlachopoulos, N. and Grätzel, M. (1993). Conversion of light to electricity by cis-X2bis (2, 2'-bipyridyl-4, 4'-dicarboxylate) ruthenium (II) charge-transfer sensitizers (X= Cl^-, Br^-, I^-, CN^-, and SCN^-) on nanocrystalline titanium dioxide electrodes. *Journal of the American Chemical Society*. **115**(14): 6382-6390.

O'Regan, B. and Grätzel, M. (1991). A low-cost, high-efficiency solar cell based on dye-sensitized colloidal TiO_2 films. *Nature*. **353**(6346): 737-740.

Oprea, C. I., Frecuş, B., Minaev, B. F. and Gîrţu, M. A. (2011). DFT study of electronic structure and optical properties of some Ru-and Rh-based complexes for dye-sensitized solar cells. *Molecular Physics*. **109**(21): 2511-2523.

Peter, L. (2007). Characterization and modeling of dye-sensitized solar cells. *American Chemical Society Transactions*. **6**(2): 555-565.

Polo, A.S. and Iha, N. Y. M. (2006). Blue sensitizers for solar cells: natural dyes from Calafate and Jaboticaba. *Solar Energy Materials and Solar Cells*. **90**(13): 1936-1944.

Roy, M., Balraju, P., Kumar, M. and Sharma, G. (2008). Dye-sensitized solar cell based on Rose Bengal dye and nanocrystalline TiO_2. *Solar Energy Materials and Solar Cells*. **92**(8): 909-913.

Rudolph, M., Yoshida, T., Miura, H. and Schlettwein, D. (2015). Improvement of Light Harvesting by Addition of a Long-Wavelength Absorber in Dye-Sensitized Solar Cells Based on ZnO and Indoline Dyes. *The Journal of Physical Chemistry*. **119**(3): 1298-1311.

Sacco, A., Rolle, L., Scaltrito, L., Tresso, E. and Pirri, C. F. (2013). Characterization of photovoltaic modules for low-power indoor application. *Applied Energy*. **102**(1295-1302.

Santhanamoorthi, N., Lo, C. M. and Jiang, J. C. (2013). Molecular design of porphyrins for dye-sensitized solar cells: a DFT/TDDFT study. *The Journal of Physical Chemistry Letters*. **4**(3): 524-530.

Sayama, K., Tsukagoshi, S., Hara, K., Ohga, Y., Shinpou, A., Abe, Y., Suga, S. and Arakawa, H. (2002). Photoelectrochemical properties of J aggregates of benzothiazole merocyanine dyes on a nanostructured TiO_2 film. *The Journal of Physical Chemistry B*. **106**(6): 1363-1371.

Schmidt, M. W., Baldridge, K. K., Boatz, J. A., Elbert, S. T., Gordon, M. S., Jensen, J. H., Koseki, S., Matsunaga, N., Nguyen, K. A. and Su, S. (1993). General atomic and molecular electronic structure system. *Journal of Computational Chemistry*. **14**(11): 1347-1363.

Schulz, H. and Baranska, M. (2007). Identification and quantification of valuable plant substances by IR and Raman spectroscopy. *Vibrational Spectroscopy*. **43**(1): 13-25.

Sekar, N. and Gehlot, V. Y. (2010). Metal Complex Dyes for Dye-Sensitized Solar Cells: Recent Developments. *Resonance*.**15**(9):819-831

Shalini, S., Balasundara prabhu, R., Prasanna, S., Mallick, T. K. and Senthilarasu, S. (2015). Review on natural dye sensitized solar cells: Operation, materials and methods. *Renewable and Sustainable Energy Reviews*. **51**(1306-1325.

Syafinar, R., Gomesh, N., Irwanto, M., Fareq, M. and Irwan, Y. (2015). Chlorophyll pigments as nature based dye for dye-sensitized solar cell (DSSC). *Energy Procedia*. **79**(896-902.

Tennakone, K., Kumarasinghe, A., Kumara, G., Wijayantha, K. and Sirimanne, P. (1997). Nanoporous TiO_2 photoanode sensitized with the flower pigment cyanidin. *Journal of Photochemistry and Photobiology*. **108**(2-3): 193-195.

Tokarev, K. L. (2007-2009). OpenThermo v.1.0 Beta 1 (C) ed. Retrieved from http://openthermo.software.informer.com/.

Wang, Z. S., Hara, K., Dan-oh, Y., Kasada, C., Shinpo, A., Suga, S., Arakawa, H. and Sugihara, H. (2005). Photophysical and (photo) electrochemical properties of a coumarin dye. *The Journal of Physical Chemistry*. **109**(9): 3907-3914.

Wongcharee, K., Meeyoo, V. and Chavadej, S. (2007). Dye-sensitized solar cell using natural dyes extracted from rosella and blue pea flowers. *Solar Energy Materials and Solar Cells*. **91**(7): 566-571.

Xu, J., Zhang, H., Liang, G., Wang, L., Weilin, X., Cui, W. and Zengchang, L. (2010). DFT Studies on the electronic structures of indoline dyes for dye-sensitized solar cells. *Journal of the Serbian Chemical Society*. **75**(2): 259-269.

Yamazaki, E., Murayama, M., Nishikawa, N., Hashimoto, N., Shoyama, M. and Kurita, O. (2007). Utilization of natural carotenoids as photosensitizers for dye-sensitized solar cells. *Solar Energy*. **81**(4): 512-516.

Yella, A., Lee, H. W., Tsao, H. N., Yi, C., Chandiran, A. K., Nazeeruddin, M. K., Diau, E. W. G., Yeh, C. Y., Zakeeruddin, S. M. and Grätzel, M. (2011). Porphyrin-sensitized solar cells with cobalt (II/III)–based redox electrolyte exceed 12 percent efficiency. *Science*. **334**(6056): 629-634.

Zhang, L. and Cole, J. M. (2015). Anchoring groups for dye-sensitized solar cells. *American Chemical Society Applied Mater Interfaces*. **7**(6): 3427-3455.

Zhou, H., Wu, L., Gao, Y. and Ma, T. (2011). Dye-sensitized solar cells using 20 natural dyes as sensitizers. *Journal of Photochemistry and Photobiology*. **219**(2): 188-194.

Zhurko, G. A. and Zhurko, D. A. (2015). Chemcraft. Version 1.7 (build 132). Retrieved from HTML:www.chemcraftprog.com.

RESEARCH OUTPUT

Journal Artilcle

Paper 1: Combination of Natural Dye (Crocetin) and Sythetic Dye (Indoline D205) for DSSCs Application.

Msangi, A., Pogrebnoi, A., Pogrebnaya, T. (2018). Combination of Natural Dye (Crocetin) and Sythetic Dye (Indoline D205) for DSSCs Application. Journal of Computational and Theoretical Chemistry. **6**(1): 1-13.

International Journal of Computational and Theoretical Chemistry
2018; 6(1): 1-13
http://www.sciencepublishinggroup.com/j/ijctc
doi: 10.11648/j.ijctc.20180601.11
ISSN: 2376-7286 (Print); ISSN: 2376-7308 (Online)

Combination of Natural Dye (Crocetin) and Synthetic Dye (Indoline D205) for DSSCs Application

Abdala Msangi*, Alexander Pogrebnoi, Tatiana Pogrebnaya

Department of Materials, Energy Science and Engineering, The Nelson Mandela African Institution of Science and Technology, Arusha, Tanzania

Email address:
msangia@nm-aist.ac.tz (A. Msangi), alexander.pogrebnoi@nm-aist.ac.tz (A. Pogrebnoi), tatiana.pogrebnaya@nm-aist.ac.tz (T. Pogrebnaya)
*Corresponding author

To cite this article:
Abdala Msangi, Alexander Pogrebnoi, Tatiana Pogrebnaya. Combination of Natural Dye (Crocetin) and Synthetic Dye (Indoline D205) for DSSCs Application. *International Journal of Computational and Theoretical Chemistry*. Vol. 6, No. 1, 2018, pp. 1-13.
doi: 10.11648/j.ijctc.20180601.11

Received: November 30, 2017; **Accepted**: December 8, 2017; **Published**: January 19, 2018

Abstract: Dye-sensitized solar cells (DSSCs) are reckoned as emerging next-generation solar cells of a high potency. Co-sensitization of dyes facilitates widening of the light absorption range of a sensitizer and is one of possible options to improve overall DSSC performance. In this work, an effect of combination of the natural crocetin dye and synthetic metal free indoline D205 dye was studied. Molecular design of a complex formed from the individual dyes was attempted. The structures, vibrational and electronic spectra of the species were computed by DFT and TD-DFT B3LYP5 methods with mid-sized basis sets. The UV-vis absorption spectra were measured for individual dyes and their mixture in chloroform solutions. Electron density distribution of the frontier molecular orbitals and energy levels alignment were used for analysis of the electronic spectra and mechanism of transitions. The results indicated that the designed complex can be considered as a potential candidate for DSSCs application with improved properties compared to the individual dyes.

Keywords: Dye-Sensitized Solar Cells (DSSCs), IR and UV-Vis Spectra, Time-Dependent Density Functional Theory (TD-DFT), Crocetin, Indoline D205

1. Introduction

Dye-sensitized solar cells (DSSCs) are regarded as low cost next-generation solar cells, and significant progress has been made in their performance and stability since their discovering in 1991 by Michael Grätzel and Brian O'Regan [1]. Among the components of DSSC, the sensitizer is a crucial part as this mimic the function of chlorophyll in plant due to the fact that it significantly influences on the power conversion efficiency as well as the stability of the devices [2]. To date, the most efficient DSSCs are made using ruthenium dye complexes with reported power conversion efficiency of about 12% at the illumination of 100 mW cm^{-2} (AM 1.5) [2-4]. Researchers have tested different types of sensitizers, including natural and synthetic dyes, so as to identify their ability to convert light into electricity. However, the DSSCs fabricated using natural dyes suffer from very low efficiencies [5] while the synthetic dyes are expensive in terms of synthetic route and utilization of heavy transition metals [6, 7].

Experimental and theoretical studies of physical and chemical properties of dyes contribute to understanding of the relationship between structure, properties of dyes and performance of a solar cell and hence facilitate design and synthesis of novel dyes for DSSCs application [8-13]. Many efforts were focused on synthesis of suitable donor-acceptor dyes, design of solar cells with novel materials and architectures [14, 15]. For a dye to be useful in DSSC, the important criteria include the electron-donating part [16, 17], a unit to adjust the absorption spectrum [18], and the electron-acceptor part [19]. Combinations of dyes with shorter and longer wavelengths absorption were investigated aimed to increase the light absorption range and hence improve overall solar cell performance [20-23]. To our knowledge, no work about the combination of natural and synthetic dyes was reported in literature by now.

The aim of this work is to study an effect of combination of natural crocetin dye and synthetic metal free dye indoline

D205 considering them as sensitizers in DSSCs. The experimental part comprises measurements and analysis of UV-vis spectra of the individual dyes' solutions and their mixture. The theoretical part includes the computations of the vibrational and electronic spectra of the crocetin and indoline D205 molecules as well as a complex designed through combination of individual dyes.

2. Materials and Methods

2.1. Experimental Details

The crocetin and indoline D205 dye samples were purchased in powder form with a stated purity of 97% (HPLC) from MedKoo Biosciences, Inc (USA) and Sigma-Aldrich Chemical Company (USA), respectively; and were used without further purification for solution preparation at room temperature.

For crocetin solution preparation, 0.7 mg of the crocetin powder was dissolved in 10 ml (7×10^{-2} g L^{-1}) of chloroform, and then 1 ml of the solution was added to 5 ml of chloroform resulting in 1.4×10^{-2} g L^{-1} concentration. This was used as a sample for crocetin Uv-vis spectra measurements. Also for indoline dye D205, 0.5 mg of the sample was dissolved in 50 ml of chloroform resulting in concentration 10^{-2} g L^{-1}, then 1 ml of this solution was added to 40 ml of chloroform, and the solution of indoline used for Uv-vis spectra measurements had the concentration of 2.5×10^{-4} g L^{-1}. For the mixture preparation, 1 ml of the indoline dye D205 solution was added to 1 ml of crocetin dye solution. This was used as a sample for measurements of UV-vis spectra. The UV-vis spectra of the samples prepared have been recorded in the region around 200–800 nm using a single beam 2800 UV-vis spectrophotometer (Hitachi U-2000).

2.2. Computational Details

The density functional theory B3LYP5 with 3-21G basis set was used for the geometrical parameters optimization and computation of vibrational spectra. The initial coordinates of the crocetin $C_{20}H_{24}O_4$ and indoline D205 $C_{48}H_{47}N_3O_4S_2$ molecules were taken from Chem Spider [24]. The complex $C_{68}H_{69}N_3O_7S_2$ was designed through combination (etherification) of these two molecules. For the computation of the complex parameters the same approach, B3LYP5/3-21G, as for individual dyes was applied. The energy and enthalpy of the complex formation reaction

$$C_{20}H_{24}O_4 + C_{48}H_{47}N_3O_4S_2 = C_{68}H_{69}N_3O_7S_2 + H_2O \quad (1)$$

were computed with different basis sets, from 3-21G to 6-31G (d, p) with geometrical parameters optimized with the 3-21G basis set. The energies of the reaction $\Delta_r E$ were calculated as the difference between the total energies of the product and reactants:

$$\Delta_r E = \Sigma E_{prod} - \Sigma E_{react} \quad (2)$$

The enthalpies of the reactions $\Delta_r H°(0)$ were obtained using $\Delta_r E$ and the zero-point vibration energy $\Delta_r \varepsilon$:

$$\Delta_r H°(0) = \Delta_r E + \Delta_r \varepsilon \quad (3)$$

$$\Delta_r \varepsilon = \frac{1}{2} hc\,(\Sigma\omega_{i\ prod} - \Sigma\omega_{i\ react}) \quad (4)$$

where h is the Plank's constant, c is the speed of light in the free space, $\Sigma\omega_{i\ prod}$, and $\Sigma\omega_{i\ react}$ are the sums of the vibration frequencies of the product and reactants, respectively.

The electronic spectra of the species both for vacuum and solvent (chloroform) were calculated at the TD-DFT B3LYP5/6-31G level of theory. The calculations were performed using the Firefly QC package [25], which is partially based on the GAMESS (US) [26] source code. The geometrical structures, vibrational and electronic spectra were visualized and analyzed using the Chemcraft [27] and Mac Mol Plt [28] software.

3. Results and Discussion

3.1. Molecular Structure of Individual Dyes and Complex

Equilibrium geometrical structures of crocetin and indoline molecules are shown in Figures 1, 2. In the crocetin, the middle part is composed of four methyl groups, and two carboxylic groups COOH attached at the ends. The molecular structure of the indoline dye D205 comprises diphenylethenyl, bicyclic indoline and two rhodanine groups [29]. The combination of two dyes through the chemical reaction (1) with elimination of water molecule leads to the formation of the complex; the optimized geometrical structure is shown in Figure 3. The selected geometrical parameters of the individual dyes are compared with those in the complex molecule in Tables 1, 2.

In the complex, the joining of the molecules occurs *via* a new chemical bond C19-O3-C23. One can suggest that formation of this bond is accompanied by detachment of the H-atom from H23-O1-C19 fragment of the crocetin (Figure 1) and hydroxyl O2-H3 from the carboxylic group of the indoline (Figure 2) to release water molecule. The bond C19-O3-C23 in the complex is specified with parameters R(C19-O3) = 1.461 Å, R(O3-C23) = 1.385 Å, ∠C19-O3-C23 = 119.2°; which are comparable with those of the ether C-O-C linkage, 1.40 Å and 110°. In the vicinity of the new chemical bond, a slight elongation of the internuclear distances C-O and C=C, by 0.003–0.069 Å, is observed while the bond lengths C=O and C-C are slightly decreased. Generally, from individual dyes to the complex, the difference in the respective parameters is in the range from –0.02 Å to +0.07 Å for bond lengths and ±0.05° for bond angles; bigger change is seen for crocetin moiety. The parameters of the remote parts of the complex remain practically the same as within the individual dyes.

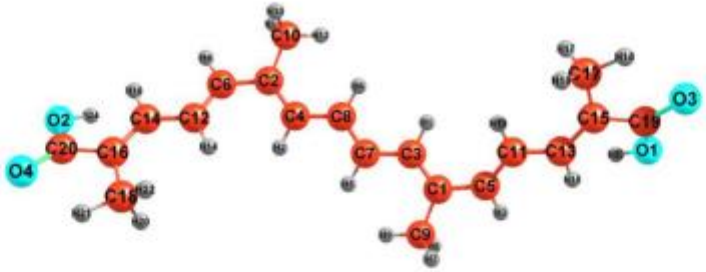

Figure 1. Optimized geometrical structure of the crocetin molecule.

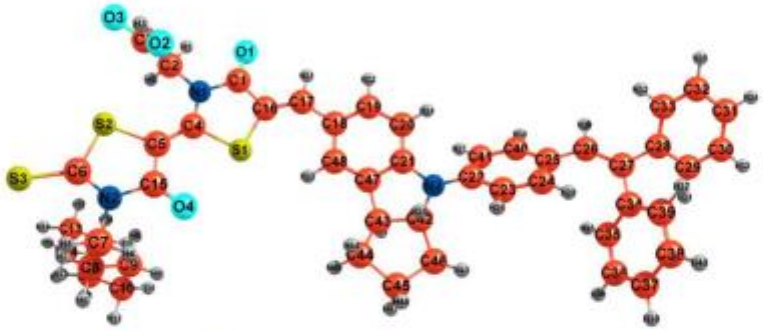

Figure 2. Optimized geometrical structure of the indoline dye D205 molecule.

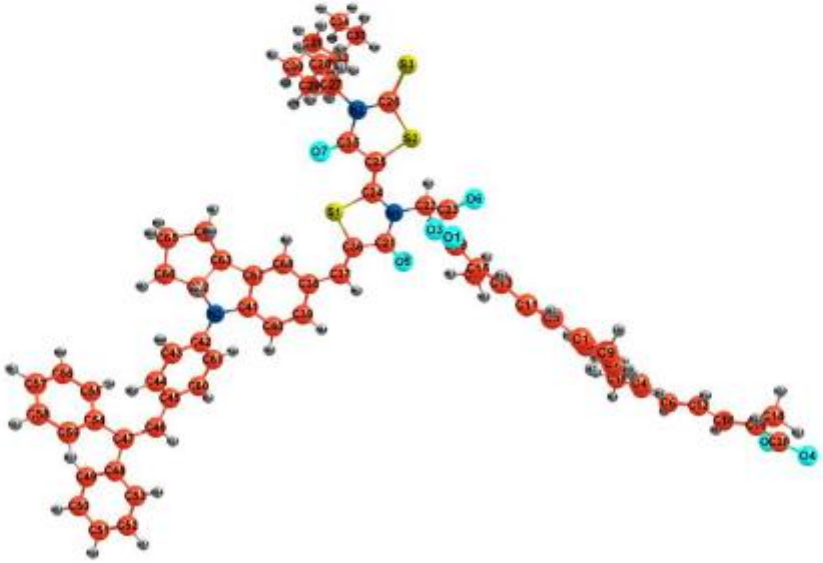

Figure 3. Optimized geometrical structure of the complex molecule.

Table 1. *Comparison of selected geometrical parameters in crocetin and complex molecules.*

Crocetin		Complex		Difference
Bond lengths, Å				
O3=C19	1.226	O1=C19	1.217	−0.009
O1-C19	1.392	O3-C19	1.461	+0.069
		O3-C23	1.385	
C15-C19	1.493	C15-C19	1.470	−0.023
C13=C15	1.356	C13=C15	1.361	+0.005
C11-C13	1.441	C11-C13	1.434	−0.007
C1-C5	1.458	C1-C5	1.455	−0.003
C16-C20	1.493	C16-C20	1.493	0.000
O4=C20	1.226	O4=C20	1.226	0.000
Bond angles, deg				
O1-C19=O3	119.5	O3-C19=O1	118.8	−0.7
C17-C15-C19	114.5	C17-C15-C19	119.9	+5.4
C13=C15-C19	120.3	C13=C15-C19	114.9	−5.4
C1-C5=C11	127.0	C1-C5=C11	128.3	+1.3
C18-C16-C20	114.5	C18-C16-C20	114.3	−0.2
O2-C20=O4	119.5	O2-C20=O4	119.5	0.0

Table 2. *Comparison of selected geometrical parameters in indoline D205 and complex molecules.*

Indoline D205		Complex		Difference
Bond lengths, Å				
C2-C3	1.523	C22-C23	1.525	+0.002
N1-C2	1.465	N1-C22	1.463	−0.002
C4=C5	1.355	C24 =C25	1.358	+0.003
C1-C16	1.459	C21-C36	1.458	−0.001
C3-O2	1.372	C23-O3	1.385	+0.013
C3=O3	1.222	C23=O6	1.219	−0.003
C1=O1	1.238	C21=O5	1.241	+0.003
C17-C18	1.444	C37-C38	1.444	0.000
C16=C17	1.351	C36=C37	1.352	+0.001
S1-C4	1.848	S1-C24	1.846	−0.002
C19=C20	1.392	C39=C40	1.393	+0.001
C21-N3	1.409	C41-N3	1.407	−0.002
C35=C36	1.398	C55=C56	1.396	−0.002
Bond angles, deg				
C3-C2-N1	114.4	C23-C22-N1	113.9	−0.5
S2-C6=S3	122.0	S2-C26=S3	121.9	−0.1
C4=C5-S2	127.7	C24=C25-S2	128.1	+0.4
C4-S1-C16	89.7	C24-S1-C36	89.7	0.0
C16=C17-C18	131.5	C36=C37-C38	131.2	−0.3
Dihedral angles, deg				
C15-N2-C6-S3	178.9	C35-N2-C26-S3	179.4	+0.5
S1-C4-C5-S2	178.6	S1-C24-C25-S2	177.2	−1.4

The thermodynamic characteristics of the complex formation reaction (1) are given in Table 3. The thermodynamic functions, entropies $S^\circ(T)$ and enthalpy increments $H^\circ(T)–H^\circ(0)$, of the crocetin, indoline, complex and water molecules have been computed with OpenThermo software [30]; in calculations, the geometrical parameters and vibrational frequencies of the molecules were used as computed with the 3-21G basis set. The Gibbs free energies $\Delta_r G^\circ(T)$ of the reaction were calculated as follows:

$$\Delta_r G^\circ(T) = \Delta_r H^\circ(T) - T\Delta_r S^\circ(T) \qquad (5)$$

where $\Delta_r H^\circ(T)$ and $\Delta_r S^\circ(T)$ are the enthalpy and entropy of the reaction at temperature T; $\Delta_r H^\circ(T) = \Delta_r H^\circ(0) + \Delta_r[H^\circ(T)–H^\circ(0)]$.

Table 3. *The thermodynamic characteristics of reaction (1): energy $\Delta_r E$, zero point vibration energy $\Delta_r\varepsilon$, enthalpies $\Delta_r H^\circ(0)$ and $\Delta_r H^\circ(298)$, Gibbs free energy $\Delta_r G^\circ(298)$.*

Quantity, kJ mol^{-1}	3-21G	6-31G	6-31G (d, p)
$\Delta_r E$	42.2	41.5	41.9
$\Delta_r\varepsilon$	–8.83	(–8.83)	(–8.83)
$\Delta_r H^\circ(0)$	33.4	32.7	33.1
$\Delta_r H^\circ(298)$	38.1	36.4	36.8
$\Delta_r G^\circ(298)$	48.2	46.5	46.9

The values of $\Delta_r E$ computed with different basis sets do not change noticeably with the basis set extension. Positive values of enthalpies $\Delta_r H^\circ$ show endothermicity of the reaction. The entropy of the reaction is negative, $\Delta_r S^\circ$ (298) = –33.9 J mol^{-1} K^{-1}, that points out a rising of the system's order. The Gibbs energy being positive at 298 K shows non-spontaneity of the complex formation through direct combination of the dyes' molecules.

3.2. Vibrational Spectra of the Species

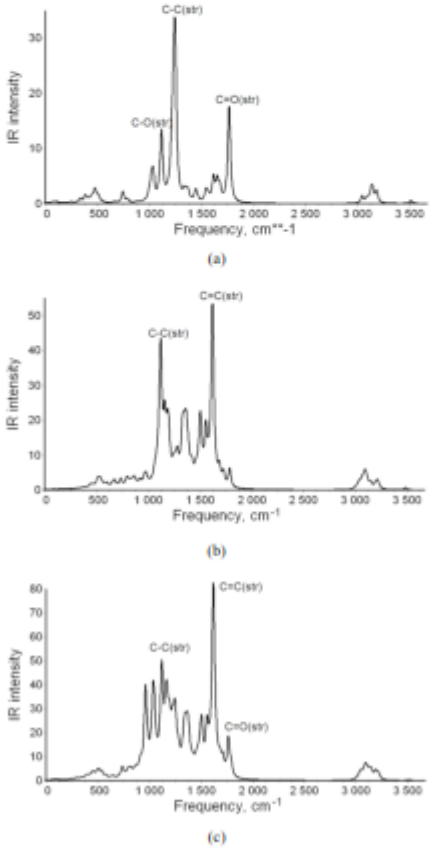

Figure 4. *IR spectra: (a) crocetin; (b) indoline D205; (c) complex.*

Vibrational spectra of the species were calculated by DFT B3LYP5 method with 3-21G basis set. An absence of imaginary frequencies confirmed that the geometrical structures of the species corresponded to minima on the potential energy surfaces. The computed IR spectra are shown in Figure 4. The most intensive modes in the spectra are assigned to the vibrations 1220-1247 cm^{-1} (C-C stretching), 1615-1676 cm^{-1} (C=C stretching), 1115 cm^{-1} (C-O stretching and CH_3 bending), 1764 cm^{-1} (C=O stretching) of the crocetin molecule, and 1120 cm^{-1} (C-C stretching), 1618-1621 cm^{-1} (C=C stretching), 1156-1188 cm^{-1} (mostly C-N and C-C stretching), 1504 cm^{-1} and 1556 cm^{-1} (H-C-H bend in the six-member ring), 1786 cm^{-1} (C=O stretching) of the indoline molecule. Comparison of our results to experimental frequencies of crocetin [31], 1536 cm^{-1} (C=C stretching), 1165 cm^{-1} (C-C stretching) and 1020 cm^{-1} (C-C in-plane rocking), shows that our calculated frequencies are overrated by 7-8% which is typical for theoretical results of similar computational level.

IR spectrum of the complex (Figure 4c) apparently comprises the intensive modes which correspond to the crocetin moiety (1115 cm^{-1} C-O stretching and CH_3 bending, 1251 cm^{-1} C-C stretching), and indoline moiety (1121 cm^{-1} C-C stretching, 1154 cm^{-1} C-N and C-C stretching, 1616-1619 cm^{-1} C=C stretching) being shifted slightly from the position in spectra of individual dyes. The frequencies in the range 1760-1790 cm^{-1} relate to stretching vibrations of two C=O groups, one from crocetin and another from indoline part. Also one can see the additional picks at 960 and 1167 cm^{-1} which are assigned to the C-O stretching motion of atoms in the new bond C19-O3-C23 between the moieties.

3.3. Electronic Spectra of the Species

For the three molecules under study, the electronic spectra were computed for vacuum and for chloroform solution using polarized continuum model. The vertical excitation energies (E_{ex}), wavelengths (λ), oscillator strengths (f) and electronic configurations of the transitions are listed in Table 4. The singlet–singlet ($S_0 \rightarrow S_{ex}$) excitations with nonzero oscillator strengths ($f > 0.001$) were taken into account.

In spectra of all species the bands of maximum wavelengths are seen in visible region. For the crocetin and indoline molecules, the excitations from the ground to first excited state are of the highest oscillator strength and attributed to the HOMO-LUMO (H→L) transitions while for the complex the more probable transitions are to the second and third excited states and assigned mostly to H→L+1 and H–1→L.

Table 4. Electronic spectra of crocetin, indoline D205 and complex molecules (TD-DFT B3LYP5/6-31G).

No of excited state	E_{ex}, eV	λ, nm	f	Electronic transition configuration
Crocetin, vacuum				
1	2.53	490	1.882	H→L, 88→89
3	3.82	325	0.050	H–1→L, 87→89
5	3.87	321	0.021	H–3→L, 85→89
6	3.93	316	0.053	H→L+2, 88→91
7	4.19	296	0.078	H–1→L+1, 87→90
9	4.80	258	0.040	H–3→L+1, 85→90
Crocetin, chloroform				
1	2.46	504	1.871	H→L, 88→89
3	3.77	329	0.066	H–1→L, 87→89
4	3.88	320	0.100	H→L+2, 88→91
5	4.10	302	0.064	H–1→L+1, 87→90
9	4.80	259	0.491	H–2→L, 86→89
Indoline D205, vacuum				
1	2.37	520	1.042	H→L, 218→219
3	2.99	414	0.567	H–1→L, 217→219
4	3.16	392	0.212	H→L+1, 218→220
5	3.39	366	0.227	H–3→L, 215→219
6	3.58	347	0.092	H→L+2, 218→221
8	3.82	325	0.068	H–1→L+1, 217→220
9	3.95	314	0.021	H-7→L, 211→219
10	3.98	311	0.023	H-4→L, 214→219
Indoline D205, chloroform				
1	2.16	574	0.807	H→L, 218 →219
2	2.84	436	0.582	H–1→L, 217→219
3	2.95	421	0.355	H→L+1, 218→220
5	3.34	371	0.126	H–2→L, 216→219
6	3.53	351	0.343	H→L+2, 218 →221
7	3.69	336	0.030	H–1→L+1, 217→220
10	3.83	324	0.017	H-5→L, 213→219
Complex, vacuum				
1	1.99	624	0.002	H→L, 301 →302
2	2.33	531	1.666	H→L+1, 301 →303
3	2.44	509	1.741	H–1→L, 300 →302
5	2.59	479	0.001	H–2→L, 299 →302
6	2.85	435	0.003	H–3→L+1, 298 →303

No of excited state	E_{ex}, eV	λ, nm	*f*	Electronic transition configuration
Complex, chloroform				
1	2.04	606	0.002	H→L, 301 →302
2	2.13	583	1.051	H→L+1, 301 →303
3	2.16	574	0.013	H–1→L+1, 300→303
4	2.32	533	2.017	H–1→L, 300 →302

The theoretical electronic spectra of the molecules are compared to our experimental UV-vis spectra of the dyes in chloroform solutions (Figures 5-7). The theoretical results for UV-vis spectra of crocetin indicate a slight red shift of the maximum wavelength from vacuum (λ = 490 nm) to chloroform solution (λ = 504 nm). In experimental UV-vis spectrum of crocetin (Figure 5c), the broad bands are observed with maxima at 286, 412, 436, and 462 nm, the latter two are overlapping resulting in highest intensity bands. This experimental spectrum does not contradict much to the theoretical results (Figures 5 a, b) and in a good agreement with data obtained in [32] where the peaks at 415, 433 and 462 nm were observed in the visible range of the spectrum for crocetin in chloroform.

In the theoretical UV-vis spectra of indoline (Figures 6a, b), the peaks of high intensity are at 415 and 523 nm (vacuum) and at 435 and 577 nm (chloroform), thus the red shift is seen from vacuum to solution. In the experimental spectrum in chloroform (Figure 6c), the most intensive band lies in the UV region with three maxima at 288, 338, 370 nm and broad band of low intensity is observed in the range 500-600 nm. The appearance of the theoretical and experimental spectra looks different regarding intensities of the peaks, still accordance may be noted between wavelengths in spectra computed for indoline dye (523, 577 nm) and measured experimentally (~550-560 nm). Our experimental result agrees well with the value λ = 554 nm observed earlier in spectrum of indoline dye D205 in chloroform solution [33].

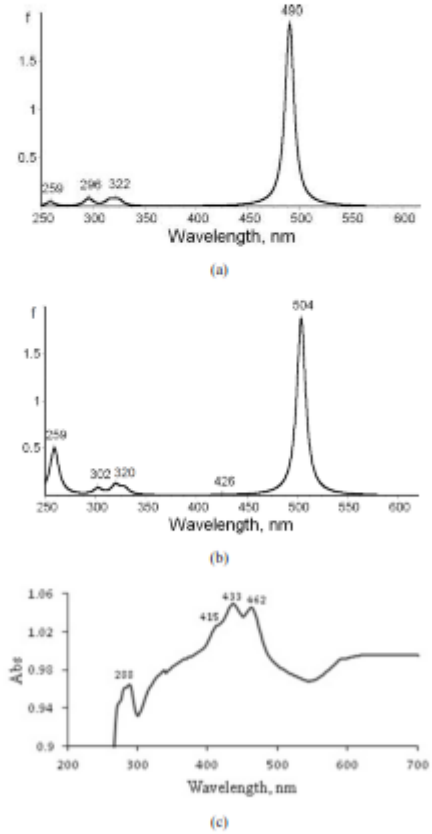

Figure 5. *UV-vis spectrum of crocetin: (a) computed for vacuum; (b) computed for chloroform solution; (c) experimental for chloroform solution.*

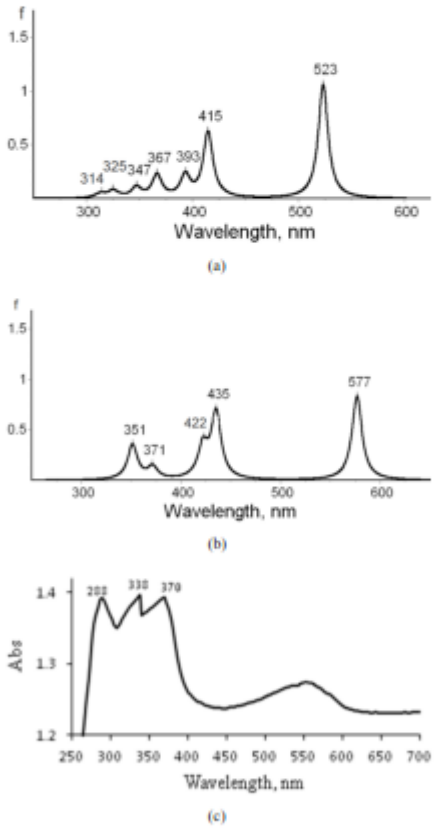

Figure 6. *UV-vis spectrum of indoline: (a) computed for vacuum; (b) computed for chloroform solution; (c) experimental for chloroform solution.*

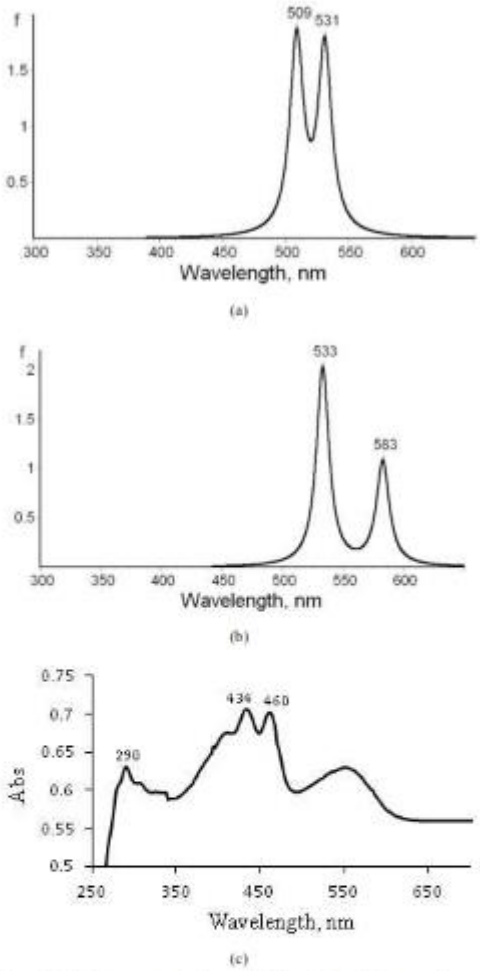

Figure 7. *UV-vis spectra of the combination of two dyes, crocetin and indoline D205: (a) computed for the complex molecule in vacuum; (b) computed for the complex molecule in chloroform solution; (c) measured experimentally for the mixture of two dyes in chloroform solution.*

The computed UV-vis spectrum of the complex contains two intensive peaks (Figures 7 a, b). Peaks at 531 nm (vacuum) and 583 nm (chloroform) correspond to those in spectra of the indoline D205 molecule: 523 and 577 nm for vacuum and chloroform, respectively. For the complex molecule, the peak at 509 nm (vacuum) or 533 nm (chloroform) does not correspond to any transition neither for crocetin nor indoline. One can suggest that this peak may relate to the new formed bond C19-O3-C23 in the complex molecule. That means that the combination of two dyes allows widening of the light adsorption in visible range and thus improving the sensitizing ability of the dye.

In the experimental measurements of UV-vis spectrum of the mixture (Figure 7c), four maxima were identified, three in visible region (434, 460 and ~550 nm) and one in ultraviolet (290 nm). Two peaks among them resemble those in spectrum of individual crocetin, 436 and 462 nm (Figure 5c) while the other two peaks correspond to those in spectrum of individual indoline dye D205, 288 and ~554 nm (Figure 6c). If compare the theoretical spectrum of the complex molecule and experimental for the mixture, one can see that two sharp peaks in the former look like merged into one broaden band in the latter. However no strong evidence of chemical interaction between individual dyes in solution is noticed. This observation is in accordance with the conclusion based on thermodynamic approach (Table 3) that the reaction (1) of complex formation is not thermodynamically favorable being endothermic and non-spontaneous.

3.4. Analysis of Frontier Molecular Orbitals and Energy Levels Alignment

Useful information about electronic structure of molecules and mechanisms of chemical reactions can be revealed from analysis of molecular orbitals [34, 35]. For the crocetin and indoline D205 molecules in vacuum, the frontier orbitals isosurfaces and energies are shown in Figures 8, 9. The number of occupied orbitals is 88 for crocetin and 218 for indoline molecules. From the shape of the orbitals, it is seen that in crocetin, both HOMO and LUMO are delocalized and electron density is distributed along the carbon chain. In indoline, the frontier orbitals are more localized; HOMO is located mostly on the diphenylethenyl part and on the indoline ring and LUMO on the rhodanine rings. In the electronic spectra of both molecules, the excitation $S_0 \rightarrow S_1$ is specified with high oscillator strengths (Table 4), and HOMO→LUMO transition contributes mostly to this first excited state transition.

The frontier and adjacent orbitals (HOMO, LUMO, H–1, and L+1) of the complex molecule in vacuum are displayed in Figure 10. The number of occupied orbitals is 301. The HOMO is located on the indoline part while LUMO is at the crocetin site (Figure 10a). This implies that when an electron transfers from the HOMO to LUMO, the electron density significantly decreases in the electron-donating indoline moiety, accompanied by increase in that of the electron-accepting crocetin site. Nevertheless, according to the results on oscillator strengths (Table 4), the most probable transitions are not HOMO→LUMO, but H→L+1 and H–1→L. As is observed in Figure 10b, the H–1 MO is located on the crocetin part of the complex, and L+1 MO on the indoline part. It means that the protruded picks of the electronic spectrum (Figure 7a) is attributed to the transitions within either crocetin or indoline sites in the complex molecule.

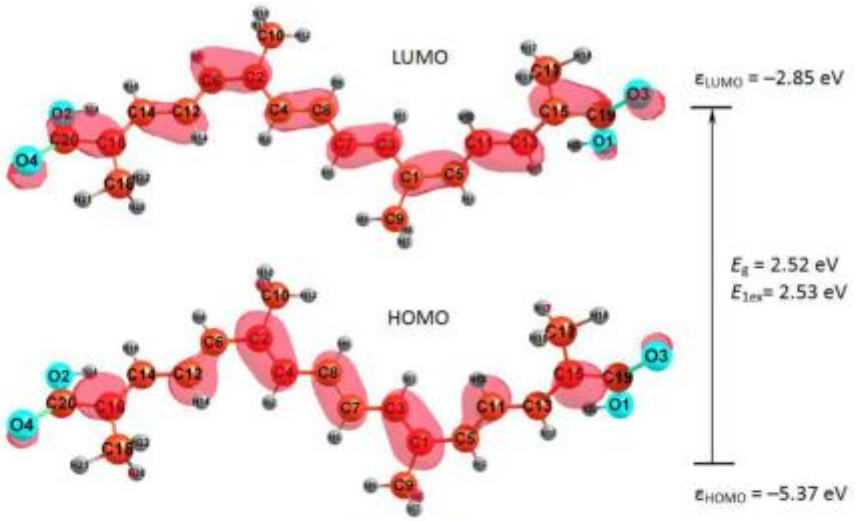

Figure 8. *Frontier orbitals HOMO and LUMO in the crocetin molecule.*

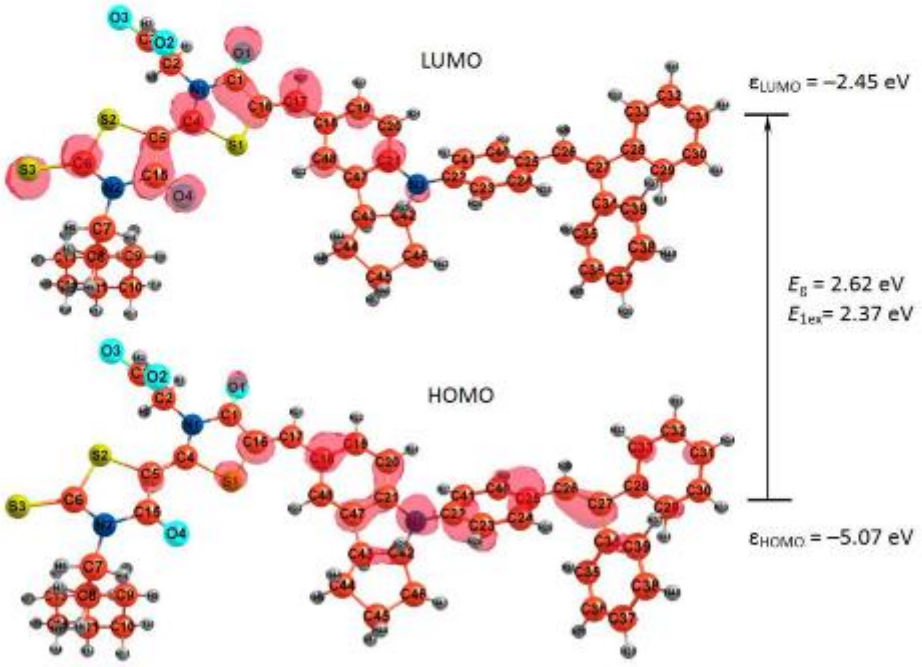

Figure 9. *Frontier orbitals HOMO and LUMO in the indoline D205 molecule.*

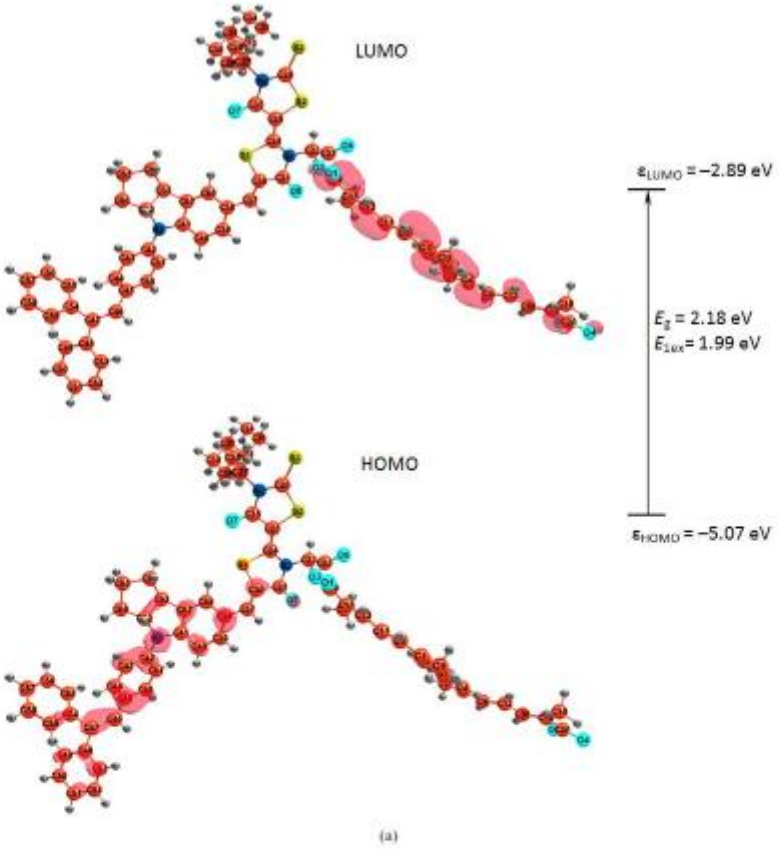
LUMO
ε_{LUMO} = −2.89 eV
E_g = 2.18 eV
E_{1ex} = 1.99 eV
HOMO
ε_{HOMO} = −5.07 eV

(a)

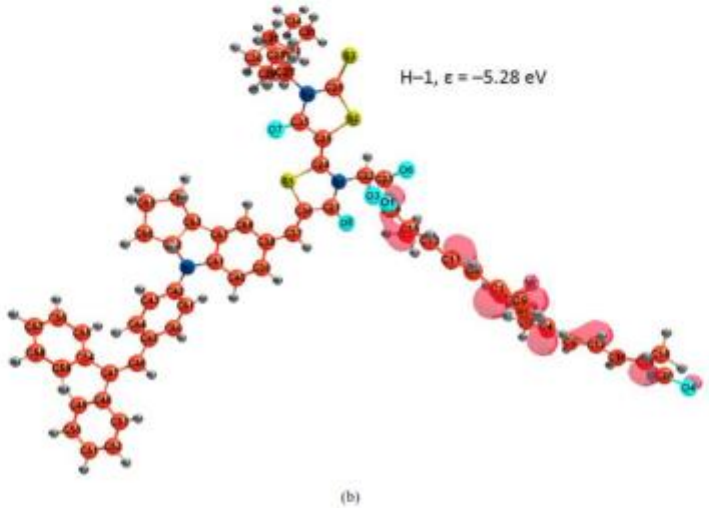
H−1, ε = −5.28 eV

(b)

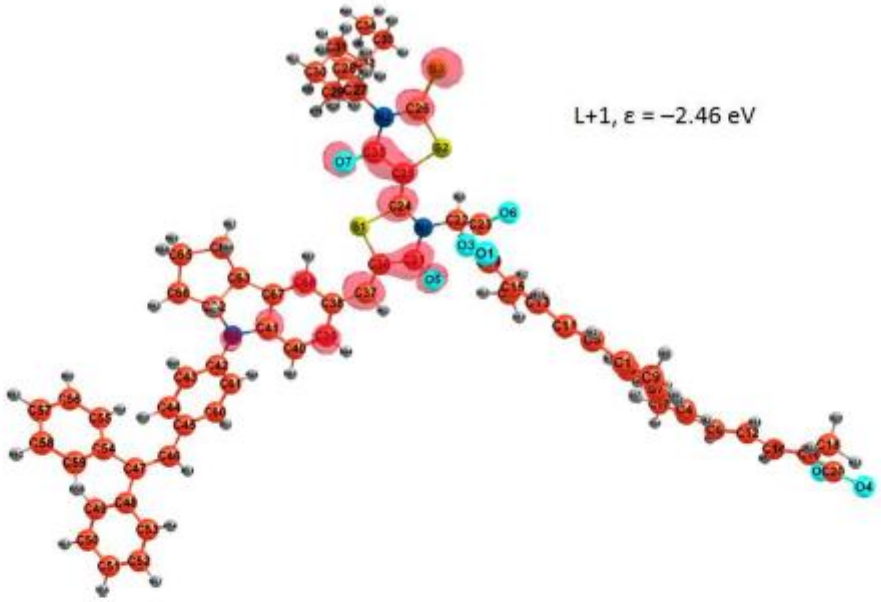

(c)

Figure 10. *Frontier and adjacent MOs in the complex molecule: (a) HOMO and LUMO; (b) H–1; (c) L+1.*

A proper energy level alignment between a dye, semiconductor and electrolyte is a fundamental requirement for a DSSC. The simplest way to consider this alignment is drawing the frontier MOs energy levels together with valence and conduction bands of a semiconductor. However more strict approach is to implement the excitation energies E_{ex} obtained by TD-DFT and calculate the excited state potentials *ESP* [36]. In our work, the values of *ESP* were found as sums of the ground state occupied MOs energies and respective excitation energies E_{ex}, $ESP = \varepsilon\,(\text{HOMO}) + E_{ex}$. The calculated energies of frontier and adjacent molecular orbitals ε(MO), excitation energies E_{ex}, energy differences between MOs E_g, and excited state potentials *ESP* are presented in Table 5. The values of E_{ex} and E_g correspond to transitions between the orbitals shown in respective column.

Although an analysis of the frontier orbitals is illustrative and useful for understanding of electron transfer mechanism, the values of excitation energies allow entire electronic spectra modeling and correct representation of electron transitions. As is seen, the values of energy gap between HOMO and LUMO (E_g) coincide with the first excitation energy (E_{ex}) for crocetin molecule; this is valid for vacuum and chloroform solution. For indoline and complex molecules, these quantities differ, the values of E_g is bigger, as a rule, the difference approaches 0.5 eV. These differences result in lowering the *ESPs* compared to respective unoccupied orbitals.

Table 5. *The energies of molecular orbitals ε(MO), excitation energies E_{ex}, energy differences between MOs E_g, and excited state potentials ESP; all values in eV.*

MO	−ε(MO)	Transition	E_{ex}	E_g	−*ESP*
Crocetin, vacuum					
88, H	5.37	H→L	2.53	2.52	2.84
89, L	2.85				
Crocetin, chloroform					
88, H	5.12	H→L	2.46	2.46	2.66
89, L	2.66				
Indoline D205, vacuum					
218, H	5.07	H→L	2.37	2.62	2.70
219, L	2.45				
Indoline D205, chloroform					
218, H	5.11	H→L	2.15	2.37	2.96
219, L	2.74				
Complex, vacuum					
300, H−1	5.28	H→L	1.99	2.18	3.08
301, H	5.07	H→L+1	2.33	2.39	2.95
302, L	2.89	H−1→L	2.44	2.91	2.63
303, L+1	2.46				
Complex, chloroform					
300, H−1	5.18	H→L	2.04	2.24	3.09
301, H	5.13	H→L+1	2.13	2.36	3.00
302, L	2.89	H−1→L	2.32	2.29	2.86
303, L+1	2.77				

The diagram in Figure 11 shows the energy levels of HOMOs and *ESPs* of the molecules under study for chloroform solutions; the valence and conduction bands of the semiconductors TiO_2 [36, 37] and ZnO [38], redox level of the I^-/I_3^- electrolyte [37, 39, 40] are given for

comparison. According to requirements, the HOMO and LUMO levels of a dye must match with the conduction-band-edge energy level of the semiconductor and the redox potential of electrolyte for an efficient charge separation and dye regeneration [41]; the HOMO level of the sensitizer has to be lower than the redox potential and the first excited state of the dye has to be slightly higher than the conduction band of the semiconductor [42, 43]. As is observed on the diagram, all three molecules meet the criteria for sensitizers: HOMO levels lie below the redox level of the electrolyte, and the excited state potentials lie above or coincide with conduction bands of semiconductors. That is the injection of electrons from the dyes to the conduction bands of TiO_2 or ZnO can occur. For the complex it is expected even higher performance due to the energy levels better meet requirements for sensitizer as the complex possesses smaller excitation energies (2.04, 2.13 and 2.32 eV for the complex compared to 2.46 eV for crocetin and 2.15 eV for indoline). Moreover, the transitions from H–1 to the first excited state and from HOMO to second excited state are of high probability to be involved in sensitizing semiconductor, and the two corresponding *ESP* levels (–2.86 and –3.00 eV) match well with the conduction band of ZnO (–2.96 eV).

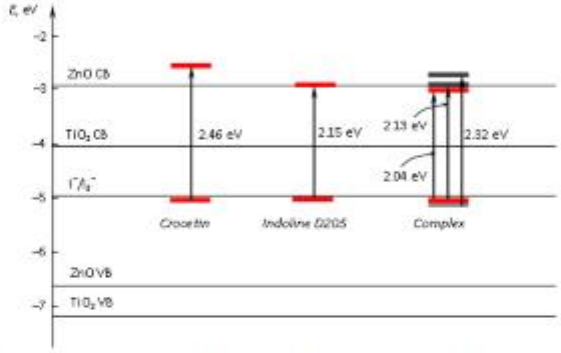

Figure 11. *Energy level diagram of HOMOs and excited state potentials of crocetin, indoline D205 and complex molecules in chloroform.*

4. Conclusion

Molecular design of solar cell sensitizer was done through the combination of two individual dyes, natural crocetin and synthetic indoline D205, aimed to improve optical properties of the materials. The properties of the complex molecule as well as individual dyes have been studied by DFT and TD-DFT methods. The equilibrium structures of the molecules, IR and electronic spectra were computed and analyzed. The thermodynamic approach indicated endothermicity and non-spontaneity of the direct joining of the components *via* C-O-C linkage. The absorption bands in experimental UV-vis spectra of the individual dyes are reproduced adequately by theoretical TD-DFT computations. The combination of two dyes results in widening of light absorption visible range and better energy level alignment with the conduction band of semiconductor ZnO and redox level of the I^-/I_3^- electrolyte. Thus the complex molecule designed might possess enhanced power conversion efficiency compared to that of individual dyes.

Acknowledgements

The authors would like to thank The British Gas (BG) Tanzania National Scholarships for the sponsorship. We also acknowledge the great help and service by the School of Life Science and Bioengineering at NM-AIST.

References

[1] B. O'Regan, M. Grätzel, A low-cost, high-efficiency solar cell based on dye-sensitized colloidal TiO_2 films, *Nature*, Vol. 353 (6346), pp. 737-740, 1991.

[2] M. K. Nazeeruddin, F. De Angelis, S. Fantacci, A. Selloni, G. Viscardi, P. Liska, S. Ito, B. Takeru, M. Grätzel, Combined experimental and DFT-TDDFT computational study of photoelectrochemical cell ruthenium sensitizers, *Journal of the American Chemical Society*, Vol. 127 (48), pp. 16835-16847, 2005.

[3] A. Hagfeldt, G. Boschloo, L. Sun, L. Kloo, H. Pettersson, Dye-sensitized solar cells, *Chemical Reviews*, Vol. 110 (11), pp. 6595-6663, 2010.

[4] M. K. Nazeeruddin, E. Baranoff, M. Grätzel, Dye-sensitized solar cells: a brief overview, *Solar Energy*, Vol. 85 (6), pp. 1172-1178, 2011.

[5] M. Miyashita, K. Sunahara, T. Nishikawa, Y. Uemura, N. Koumura, K. Hara, A. Mori, T. Abe, E. Suzuki, S. Mori, Interfacial electron-transfer kinetics in metal-free organic dye-sensitized solar cells: combined effects of molecular structure of dyes and electrolytes, *Journal of the American Chemical Society*, Vol. 130 (52), pp. 17874-17881, 2008.

[6] M. Alhamed, A. S. Issa, A. W. Doubal, Studying of natural dyes properties as photo-sensitizer for dye sensitized solar cells (DSSC), *Journal of Electron Devices*, Vol. 16 (11), pp. 1370-1383, 2012.

[7] G. P. Smestad, M. Gratzel, Demonstrating electron transfer and nanotechnology: a natural dye-sensitized nanocrystalline energy converter, *Journal of Chemical Education,* Vol. 75 (6), pp. 752, 1998.

[8] H. W. Ham, Y. S. Kim, Theoretical study of indoline dyes for dye-sensitized solar cells, *Thin Solid Films,* Vol. 518 (22), pp. 6558-6563, 2010.

[9] Z. Cai-Rong, L. Zi-Jiang, C. Yu-Hong, C. Hong-Shan, W. You-Zhi, Y. Li-Hua, DFT and TDDFT study on organic dye sensitizers D5, DST and DSS for solar cells, *Journal of Molecular Structure: THEOCHEM,* Vol. 899 (1), pp. 86-93, 2009.

[10] C.-R. Zhang, Z.-J. Liu, Y.-H. Chen, H.-S. Chen, Y.-Z. Wu, W. Feng, D.-B. Wang, DFT and TD-DFT study on structure and properties of organic dye sensitizer TA-St-CA, *Current Applied Physics,* Vol. 10 (1), pp. 77-83, 2010.

[11] T. Ruiz-Anchondo, N. Flores-Holguin, D. Glossman-Mitnik, Natural carotenoids as nanomaterial precursors for molecular photovoltaics: a computational DFT study, *Molecules,* Vol. 15 (7), pp. 4490-4510, 2010.

[12] F. De Angelis, Direct vs. indirect injection mechanisms in perylene dye-sensitized solar cells: A DFT/TDDFT investigation, *Chemical Physics Letters,* Vol. 493 (4), pp. 323-327, 2010.

[13] N. Santhanamoorthi, C.-M. Lo, J.-C. Jiang, Molecular design of porphyrins for dye-sensitized solar cells: a DFT/TDDFT study, *The Journal of Physical Chemistry Letters,* Vol. 4 (3), pp. 524-530, 2013.

[14] A. Mishra, M. K. Fischer, P. Bäuerle, Metal-free organic dyes for dye-sensitized solar cells: From structure: Property relationships to design rules, *Angewandte Chemie International Edition,* Vol. 48 (14), pp. 2474-2499, 2009.

[15] N. Shibayama, Y. Inoue, M. Abe, S. Kajiyama, H. Ozawa, H. Miura, H. Arakawa, Novel near-infrared carboxylated 1, 3-indandione sensitizers for highly efficient flexible dye-sensitized solar cells, *Chemical Communications,* Vol. 51 (64), pp. 12795-12798, 2015.

[16] F. Zhang, Y.-h. Luo, J.-s. Song, X.-z. Guo, W.-l. Liu, C.-p. Ma, Y. Huang, M.-f. Ge, Z. Bo, Q.-B. Meng, Triphenylamine-based dyes for dye-sensitized solar cells, *Dyes and Pigments,* Vol. 81 (3), pp. 224-230, 2009.

[17] D. Casanova, F. P. Rotzinger, M. Grätzel, Computational study of promising organic dyes for high-performance sensitized solar cells, *Journal of Chemical Theory and Computation,* Vol. 6 (4), pp. 1219-1227, 2010.

[18] R. M. El-Shishtawy, Functional dyes, and some hi-tech applications, *International Journal of Photoenergy,* Vol. 2009, 2009.

[19] D. Sahu, H. Padhy, D. Patra, D. Kekuda, C.-W. Chu, I.-H. Chiang, H.-C. Lin, Synthesis and application of H-Bonded cross-linking polymers containing a conjugated pyridyl H-Acceptor side-chain polymer and various carbazole-based H-Donor dyes bearing symmetrical cyanoacrylic acids for organic solar cells, *Polymer,* Vol. 51 (26), pp. 6182-6192, 2010.

[20] D. Kuang, P. Walter, F. Nüesch, S. Kim, J. Ko, P. Comte, S. M. Zakeeruddin, M. K. Nazeeruddin, M. Grätzel, Co-sensitization of organic dyes for efficient ionic liquid electrolyte-based dye-sensitized solar cells, *Langmuir,* Vol. 23 (22), pp. 10906-10909, 2007.

[21] L. Y. Chew, H. E. Khoo, I. Amin, A. Azrina, C. Y. Lau, Analysis of phenolic compounds of dabai (Canarium odontophyllum Miq.) fruits by high-performance liquid chromatography, *Food Analytical Methods,* Vol. 5 (1), pp. 126-137, 2012.

[22] K.-M. Lee, Y.-C. Hsu, M. Ikegami, T. Miyasaka, K. J. Thomas, J. T. Lin, K.-C. Ho, Co-sensitization promoted light harvesting for plastic dye-sensitized solar cells, *Journal of Power Sources,* Vol. 196 (4), pp. 2416-2421, 2011.

[23] S. W. Park, K. Lee, D.-K. Lee, M. J. Ko, N.-G. Park, K. Kim, Expanding the spectral response of a dye-sensitized solar cell by applying a selective positioning method, *Nanotechnology,* Vol. 22 (4), pp. 045201, 2010.

[24] http://www.chemspider.com

[25] A. A. Granovsky, Firefly version 8.2.0 www http://classic.chem.msu.su/gran/firefly/index.html.

[26] M. W. Schmidt, K. K. Baldridge, J. A. Boatz, S. T. Elbert, M. S. Gordon, J. H. Jensen, S. Koseki, N. Matsunaga, K. A. Nguyen, S. Su, General atomic and molecular electronic structure system, *Journal of Computational Chemistry,* Vol. 14 (11), pp. 1347-1363, 1993.

[27] G. A. Zhurko, D. A. Zhurko, Chemcraft. Version 1.7 (build 132). Retrieved from HTML: www.chemcraftprog.com.

[28] B. M. Bode, M. S. Gordon, MacMolPlt version 7.4.2, *Journal of Molecular Graphics and Modelling*, pp. 133–138, 1998 http://www.scl.ameslab.gov/MacMolPlt/.

[29] J. Xu, H. Zhang, G. Liang, L. Wang, X. Weilin, W. Cui, L. Zengchang, DFT Studies on the electronic structures of indoline dyes for dye-sensitized solar cells, *Journal of the Serbian Chemical Society,* Vol. 75 (2), pp. 259-269, 2010.

[30] K. L. Tokarev, OpenThermo v. 1.0 Beta 1 (C) ed. http://openthermo.software.informer.com/. 2007-2009.

[31] H. Schulz, M. Baranska, Identification and quantification of valuable plant substances by IR and Raman spectroscopy, *Vibrational Spectroscopy,* Vol. 43 (1), pp. 13-25, 2007.

[32] J. B. Harbourne, Phytochemical methods: A guide to modern techniques of plant analysis, *Ghapman and Hall Ltd, London, New York,* pp. 4-120, 1984.

[33] S. Higashijima, H. Miura, T. Fujita, Y. Kubota, K. Funabiki, T. Yoshida, M. Matsui, Highly efficient new indoline dye having strong electron-withdrawing group for zinc oxide dye-sensitized solar cell, *Tetrahedron,* Vol. 67 (34), pp. 6289-6293, 2011.

[34] T. Le Bahers, T. Pauporté, G. Scalmani, C. Adamo, I. Ciofini, A TD-DFT investigation of ground and excited state properties in indoline dyes used for dye-sensitized solar cells, *Physical Chemistry Chemical Physics*, Vol. 11 (47), pp. 11276-11284, 2009.

[35] H. Lin, S.-G. Zhu, P.-Y. Chen, K. Li, H.-Z. Li, X.-H. Peng, DFT investigation of a high energy density polynitro compound, 2, 2'-Bis (trinitromethyl)-5, 5'-azo-1, 2, 3, 4-tetrazole, *Central European Journal of Energetic Materials,* Vol. 10 (3), pp. 325-338, 2013.

[36] C. I. Oprea, B. Frecuş, B. F. Minaev, M. A. Gîrţu, DFT study of electronic structure and optical properties of some Ru-and Rh-based complexes for dye-sensitized solar cells, *Molecular Physics,* Vol. 109 (21), pp. 2511-2523, 2011.

[37] F. De Angelis, S. Fantacci, A. Selloni, Alignment of the dye's molecular levels with the TiO_2 band edges in dye-sensitized solar cells: a DFT–TDDFT study, *Nanotechnology,* Vol. 19 (42), pp. 424002, 2008.

[38] T. Le Bahers, T. Pauporte, G. Scalmani, C. Adamo, I. Ciofini, A TD-DFT investigation of ground and excited state properties in indoline dyes used for dye-sensitized solar cells, *Physical Chemistry Chemical Physics*, Vol. 11 (47), pp. 11276-11284, 2009.

[39] M. W. Han, P. Ekanayake, L. C. Ming, V. N. Yoong, DFT/TD-DFT Studies on the Lawsone (Henna) as a Photosensitizer for Dye-Sensitized Solar Cells, *Applied Mechanics and Materials,* Vol. 789-790, pp. 56-60, 2015.

[40] L. Peter, Characterization and modeling of dye-sensitized solar cells, *ECS Transactions,* Vol. 6 (2), pp. 555-565, 2007.

[41] K. Hara, T. Sato, R. Katoh, A. Furube, Y. Ohga, A. Shinpo, S. Suga, K. Sayama, H. Sugihara, H. Arakawa, Molecular design of coumarin dyes for efficient dye-sensitized solar cells, *The Journal of Physical Chemistry B,* Vol. 107 (2), pp. 597-606, 2003.

[42] Z. Liu, Theoretical studies of natural pigments relevant to dye-sensitized solar cells, *Journal of Molecular Structure: THEOCHEM,* Vol. 862 (1), pp. 44-48, 2008.

[43] A. Hagfeldt, M. Graetzel, Light-induced redox reactions in nanocrystalline systems, *Chemical Reviews,* Vol. 95 (1), pp. 49-68, 1995.

Poster Presentation

INVESTIGATION OF COMBINATION EFFECT OF NATURAL DYE (CROCETIN) AND SYNTHETIC DYE (D205) FOR DYE SENSITIZED SOLAR CELLS APPLICATION

Abdala Msangi, Alexander M. Pogrebnoi, Tatiana P. Pogrebnaya
Department of Materials and Energy Science & Engineering, NM-AIST, Tanzania

Introduction

- Dye-sensitized solar cells (DSSCs) are devices for conversion of solar energy into electricity based on sensitization of wide band gap semiconductors (O'Regan and Grätzel, 1991).
- DSSCs have gained increasing attention for many years now as they present many potential advantages such as flexibility, lightweight, low cost and easy processing.
- The dye is a key component of the device since its role is to harvest efficiently the light and inject the photogenerated electrons into the semiconductor oxide.
- Many dyes, such as ruthenium complexes, zinc porphyrin and metal-free organic dyes have been extensively studied for this application.
- However the use of a single sensitizer (dye) is restricted due to wavelength range of light absorption which leads to low efficiency.
- DSSCs have been extensively investigated as potential candidates for renewable-energy systems because of their fundamental and scientific importance in the area of energy conversion (Higashijima *et al.*, 2011).

Objectives

Main Objective: The aim of this work is to investigate the effect of combination between natural dye (crocetin) and synthetic dye (indoline, D205) for DSSCs applications.

Specific Objectives:

1. Molecular design of complex molecule through combination of the crocetin and indoline D205 dyes.
2. To determine the geometrical parameters and vibrational spectra of the dyes (crocetin, tocopherol, retinol and indoline D205) by using quantum chemical methods.
3. To compute the electronic spectra of the individual dyes and complex molecule.
4. To measure experimentally UV-vis spectra of solutions of the individual dyes and mixture of selected dyes.

Significance of the research

1. This study gives foundation for the designing of a new sensitizer through a combination of natural and synthetic dyes since that, the new complex may have a high performance compared to the individual dyes.
2. Also this study lays a basis for future studies.

Methodology

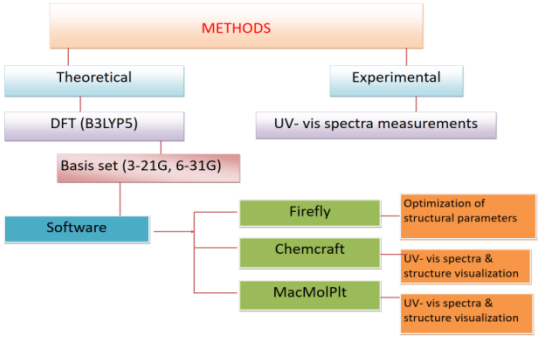

Results

(a) Molecular structure of individual dyes and complex

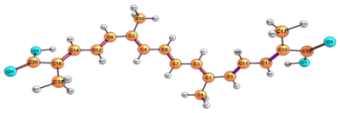

Fig. 1: Optimized geometrical structure of the crocetin ($C_{20}H_{24}O_4$).

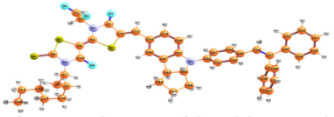

Fig. 2: Optimized geometrical structure of the indoline , D205 ($C_{48}H_{47}N_3O_4S_3$).

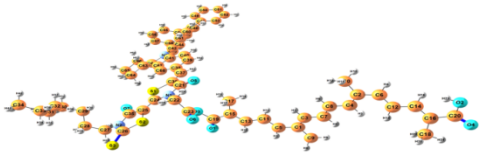

Fig. 3: Optimized geometrical structure of the complex ($C_{68}H_{69}N_3O_7S_3$).

- Equilibrium geometrical structures of crocetin and indoline molecules as well as the complex are shown in Figs. 1-3.
- The combination of two dyes through the chemical reaction ($C_{20}H_{24}O_4$ + $C_{48}H_{47}N_3O_4S_3$ = $C_{68}H_{69}N_3O_7S_3$ + H_2O) with elimination of water molecule leads to the formation of the complex.
- In the complex, the joining of the molecules occurs *via* a new chemical bond C19-O3-C23.
- One can suggest that formation of this bond is accompanied by detachment of the H-atom from H23-O1-C19 fragment of the crocetin (Fig. 1) and hydroxyl O2-H3 from the carboxylic group of the indoline (Fig. 2) to release water molecule.

(b)Theoretical UV-vis spectra

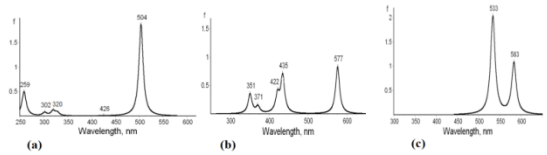

Fig. 4: Theoretical UV-vis spectra of (a) crocetin, (b) indoline, D205 (c) complex in chloroform.

- The theoretical results for UV-vis spectra of crocetin indicate a slight red shift of the maximum wavelength from vacuum (λ = 490 nm) to chloroform solution (λ = 504 nm) while for indoline red shift was 523 nm (vacuum) to 577 nm (chloroform).
- For the complex molecule, the peak at 509 nm (vacuum) or 533 nm (chloroform) does not correspond to any transition neither for crocetin nor indoline.
- One can suggest that this peak may relate to the new formed bond C19-O3-C23 in the complex molecule.

(c) Experimental UV-vis spectra

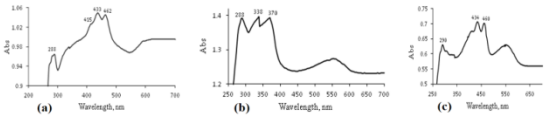

Fig. 5: Experimental UV-vis spectra of (a) crocetin, (b) indoline, D205 (c) complex.

- In experimental spectrum of crocetin (Fig. 5a), the broad bands are observed with maxima at 286, 412, 436, and 462 nm .
- This experimental spectrum does not contradict much to the theoretical results (Fig. 4 a) and in a good agreement with data obtained in (Harbourne, 1984) where the peaks at 415, 433 and 462 nm were observed in the visible range of the spectrum for crocetin in chloroform.
- Indoline D205 experimental result agrees well with the value λ = 554 nm observed earlier in spectrum of indoline dye D205 in chloroform solution (Higashijima *et al.*, 2011).

(d) Energy levels alignment

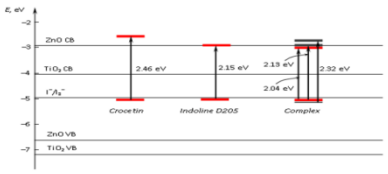

Fig. 6: Energy level diagram of HOMOs and excited state potentials of crocetin, indoline D205 and complex molecules in chloroform.

- As is observed on the diagram(Fig. 6), all three molecules meet the criteria for sensitizers: HOMO levels lie below the redox level of the electrolyte, and the excited state potentials lie above or coincide with conduction bands of semiconductors.
- For the complex it is expected even higher performance due to the energy levels better meet requirements for sensitizer as the complex possesses smaller excitation energies (2.04, 2.13 and 2.32 eV for the complex compared to 2.46 eV for crocetin and 2.15 eV for indoline).

(e) Conclusion

The molecular design of a new solar cell sensitizer was attempted through the combination of two individual dyes, natural crocetin and synthetic indoline D205, aimed to improve optical properties of the materials. The combination of two dyes results in widening of light absorption visible range and better energy level alignment with the conduction band of semiconductor ZnO and redox level of the electrolyte. Thus the complex molecule designed might possess enhanced power conversion efficiency compared to that of individual dyes.

Selected references

- O'Regan, B. and Grätzel, M. (1991). A low-cost, high-efficiency solar cell based on dye-sensitized colloidal TiO_2 films. *Nature*. **353**(6346): 737-740.
- Higashijima, S., Miura, H., Fujita, T., Kubota, Y., Funabiki, K., Yoshida, T. and Matsui, M. (2011). Highly efficient new indoline dye having strong electron-withdrawing group for zinc oxide dye-sensitized solar cell. *Tetrahedron*. **67**(34): 6289-6293.
- Harbourne, J. (1984). Phytochemical methods: A guide to modern techniques of plant analysis. *Ghapman and Hall, London*: 4-120.